Title

Seasonal cues act through the circadian clock and pigment-dispersing factor to control EYES ABSENT and downstream physiological changes

Journal

Current Biology, 33(4)

ISSN

0960-9822

Authors

Hidalgo, Sergio

Anguiano, Maribel

Tabuloc, Christine A

et al.

Publication Date

2023-02-01

DOI

10.1016/j.cub.2023.01.006

Peer reviewed

HHS Public Access

Author manuscript

Curr Biol. Author manuscript; available in PMC 2024 February 27.

Published in final edited form as:

Curr Biol. 2023 February 27; 33(4): 675–687.e5. doi:10.1016/j.cub.2023.01.006.

Seasonal cues act through the circadian clock and Pigment Dispersing Factor to control EYES ABSENT and downstream physiological changes

Sergio Hidalgo[1], **Maribel Anguiano**[1], **Christine A. Tabuloc**[1], **Joanna C. Chiu**[1,*]

[1]Department of Entomology and Nematology, College of Agricultural and Environmental Sciences, University of California, One Shields Avenue, Davis, CA 95616, USA

SUMMARY

Organisms adapt to seasonal changes in photoperiod and temperature to survive; however, the mechanisms by which these signals are integrated in the brain to alter seasonal biology are poorly understood. We previously reported that EYES ABSENT (EYA) shows higher levels in cold temperature or short photoperiod and promotes winter physiology in *Drosophila*. Nevertheless, how EYA senses seasonal cues is unclear. Pigment-Dispersing Factor (PDF) is a neuropeptide important for regulating circadian output rhythms. Interestingly, PDF has also been shown to regulate seasonality, suggesting it may mediate the function of the circadian clock in modulating seasonal physiology. In this study, we investigated the role of EYA in mediating the function of PDF on seasonal biology. We observed that PDF abundance is lower in cold and short days as compared to warm and long days, opposite of what was previously observed for EYA. We observed that manipulating PDF signaling in *eya+* fly brain neurons where EYA and PDF receptor are coexpressed modulates seasonal adaptations in daily activity rhythm and ovary development via EYA-dependent and independent mechanisms. At the molecular level, altering PDF signaling impacted EYA protein abundance. Specifically, we showed that protein kinase A (PKA), an effector of PDF signaling, phosphorylates EYA promoting its degradation, thus explaining the opposite responses of PDF and EYA abundance to changes in seasonal cues. In summary, our results support a model in which PDF signaling negatively modulates EYA levels to regulate seasonal physiology, linking the circadian clock to the modulation of seasonal adaptations.

eTOC Blurb

[*]**Corresponding author and Lead Contact**: Joanna C. Chiu, jcchiu@ucdavis.edu. Twitter handle: JCC @joanna_c_chiu.

AUTHOR CONTRIBUTIONS

S.H., C.A.T., and M.A. performed research and analyzed data; S.H. and J.C.C contributed to research conceptualization, critical interpretation of the data, and wrote the paper with the input of all the co-authors.

DECLARATION OF INTERESTS

The authors declare no competing interests.

INCLUSION AND DIVERSITY

We support inclusive, diverse, and equitable conduct of research.

Organisms adapt to seasonal changes in photoperiod and temperature to survive. Hidalgo et al. uncover a mechanism by which the circadian clock conveys these environmental cues to modulate EYES ABSENT, a protein whose expression is sensitive to seasonal cues in insects, birds, and mammals.

Graphical Abstract

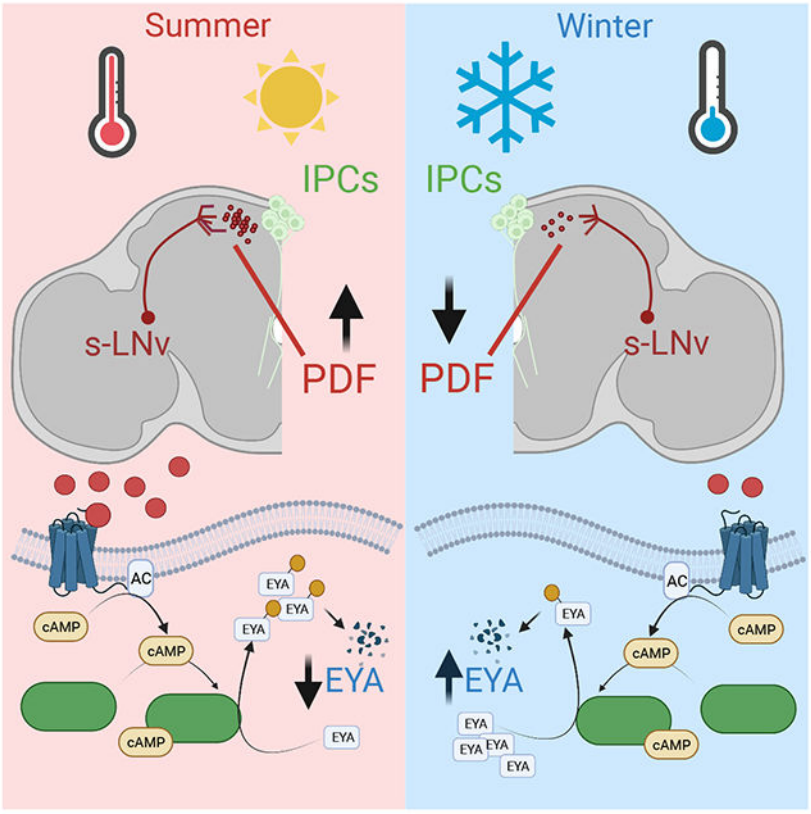

INTRODUCTION

As seasons change, organisms adapt to adverse environmental conditions to survive[1,2]. While some animals, like monarch butterflies[3,4], migrate into more favorable environments, others undergo metabolic and physiological changes that allow them to prevail through the harsh winter[5,6]. These seasonal adaptations have been described in plants[6,7] and animals[8–11], and are triggered by changes in photoperiod[12,13] (i.e. daylength) and temperature[14]. However, the molecular mechanisms that allow organisms to extract environmental information reflecting the calendar year is not well established. This is especially true in animals.

In several animals, endocrine signals drive seasonal adaptations. In mammals and birds, the increases in the hormone thyrotrophin (TSH) and the downstream T3 hormone, are key for photoperiodic summer responses[15–18]. In insects, reduction of insulin-like peptides (ILPs) and juvenile hormone (JH) are important for overwintering[19–22]. Although the hormonal

components differ between species, studies have suggested that EYES ABSENT (EYA), a cotranscription factor with phosphatase activity, could be a key conserved molecular player within the seasonal timer, acting upstream of endocrine responses to modulate seasonal physiology. In the Japanese quail (*Coturnix japonica*), the expression of the *eya* homolog, *Eya3*, increases in the *pars tuberalis* of the pituitary gland upon transitioning into summer[17]. This phenomenon is also observed in soay sheep (*Ovis aries*), where EYA3 protein has also been proposed as an effector upstream TSH-β[18,23]. We recently described a functional role of EYA in the seasonal response of *Drosophila melanogaster*[24]. Specifically, we showed that *eya* expression in the insulin-producing cells (IPCs) within the *pars intercerebralis* (*PI*), the insect ortholog of the hypothalamus, is critical for reproductive dormancy, a seasonal adaptation characterized by a reduction in ovary size and egg production. Moreover, we reported that *eya* mRNA and EYA protein levels are sensitive to changes in photoperiod and temperature, increasing in simulated winter conditions[24]. Despite evidence from multiple organisms, the mechanism mediating changes in EYA expression in response to photoperiod and temperature has yet to be determined.

The Bünning hypothesis states that the circadian clock is required for appropriate photoperiodic measurement[25,26]. The core clock in *Drosophila* is a transcriptional translational feedback loop (TTFL) composed of the positive elements CLK-CYC, which promote the transcription of the negative elements *period* (*per*) and *timeless* (*tim*) as well as other clock-regulated genes[27]. Accumulation and subsequent nuclear translocation of PER-TIM then leads to the repression of CLK-CYC activity, which in turn shuts down the transcription of *per* and *tim*, preparing the clock for the next cycle. The proteasome mediates light-dependent and light-independent degradation of the negative elements, ensuring the proper functioning and entrainment of the TTFL. Bünning proposed that circadian oscillations are composed of light and dark-requiring phases[26]. In short days, light is only present in the light phase, while in long days, light is now present in both light and in part of the dark-requiring phase. This was later modified and presented as "coincidence model"[28]. This model then assumes that the elements of the circadian clock are required for photoperiodism and seasonal adaptations. Studies in several insects have been instrumental in establishing this relationship[29–32]. Recently, Wood et al. proposed a mechanism in mammals where *Eya3* transcription is modulated by BMAL2-dependent chromatin remodeling in the *pars tuberalis* of the pituitary gland in sheep, highlighting the role of a circadian clock protein in regulating *Eya3* expression[33]. In *Drosophila* however, the IPCs do not express a functional circadian clock[34,35], although TIM expression in the fly brain is found to modulate EYA abundance[24]. This suggests that other unknown clock mechanisms must be involved in relaying environmental information to EYA-expressing cells to modulate EYA function in seasonal adaptations.

The circadian clock neuronal network provides extensive connections to and modulates the IPCs[34–38]. The clock network is composed of around 7 neuronal clusters: dorsal neurons-1 (DN1), dorsal neurons-2 (DN2), dorsal neurons-3 (DN3), lateral posterior neurons (LPN), dorsal lateral neurons (LNd), and the large and small ventral lateral neurons (l-LNvs and s-LNvs, respectively). Among clock network clusters, DN1 and s-LNvs are known to modulate the IPCs[39–41]. The s-LNvs secretes Pigment Dispersing Factor (PDF), a neuropeptide that enables the molecular synchronization of neuronal clusters within the

clock network[42,43], and is critical for the maintenance of anticipatory activity in light-dark cycles (LD) and the circadian rhythmicity in constant darkness (DD)[44–47]. Interestingly, the role of PDF in modulating seasonal adaptations has been examined in several organisms. In the blow fly and in the bean bug, ablation of the brain region containing the PDF-producing neurons prevents the discrimination between short and long photoperiod[48,49]. Moreover, ablation of *Pdf* in the brown-winged green bug impairs photoperiodic control of reproduction[50]. In *Drosophila melanogaster*, photoperiod sensitivity is lost in *Pdf* mutants[51], whereas artificially increasing or decreasing the activity of *Pdf*-expressing cells inhibits or promotes reproductive dormancy, respectively[52]. More importantly, the role of PDF in reproductive dormancy appears to be mediated by direct modulation of the IPCs[52].

Here, we explore the relationship between PDF and EYA in the context of seasonal biology. We provide evidence to support a mechanism by which PDF signaling regulates multiple aspects of seasonal physiology by conveying environmental cues to alter EYA levels in the fly brain via a PKA-dependent post-translational mechanism. We proposed that during summer-like conditions, PDF promotes EYA degradation by PKA-mediated phosphorylation, while a reduction in *Pdf* mRNA and PDF peptide in winter allows EYA accumulation, promoting winter adaptations.

RESULTS

PDF levels change with photoperiod and temperature

The circadian neuropeptide PDF is known to exhibit daily cycling in abundance in the fly brain and can be synchronized by light[53]. Furthermore, *Pdf* mRNA levels are sensitive to light intensity[54]. This suggests that PDF could be sensitive to environmental cues that change with seasons, namely photoperiod and temperature, and can subsequently convey these seasonal cues to alter EYA function in the fly brain. To test this hypothesis, we first examined the sensitivity of PDF abundance to key seasonal cues. We measured PDF levels in the dorsal terminals of the s-LNvs in flies subjected to different photoperiods and temperature conditions. First, we tested flies that were subjected to 7 days in simulated summer conditions, i.e. long photoperiod (LP, 16:8 LD) at 25°C, or simulated winter, i.e. short photoperiod (SP, 8:16 LD) at 10°C (Figure 1A–B). PDF levels showed daily rhythmicity in both conditions with peak phase at ZT0 (Rhythmicity LP25 $p = 5.4 \times 10^{-3}$, Rhythmicity SP10 $p = 3.19 \times 10^{-7}$). Although we did not observe a difference in the amplitude of PDF cycling ($p = 0.22$), a reduction in the Midline Estimating Statistic Of Rhythm (MESOR) in simulated winter compared to simulated summer was observed, suggesting an overall reduction of PDF levels in winter-like conditions (MESOR LP25 = 2.41, MESOR SP10 = 1.26, $p = 2.06 \times 10^{-17}$; Figure 1C).

To determine the effect of the photoperiod alone on PDF levels, the same experiment was conducted in flies entrained to either a long photoperiod or a short photoperiod but at constant temperature 25°C (Figure 1D–E). PDF abundance in both LP ($p = 0.005$) and SP ($p = 0.034$) were found to be rhythmic. When using CircaCompare[55], no differences in the MESOR ($p = 0.06$), amplitude ($p=0.9$) or phase ($p=0.72$) were observed between these conditions (Figure 1F). Interestingly, the peak estimated for SP by CircaCompare was ZT1.5, far from the ZT4 peak based on visual inspection of the data. We therefore confirmed

the phase of the peak using Rhythmicity Analysis Incorporating Nonparametric methods (RAIN)[56]. Compared to CircaCompare, RAIN is better suited for detection of peaks in skewed waveforms, as in the case for SP25°C (Figure 1F). While CircaCompare and RAIN were in agreement when computing the phases for all other datasets in Figure 1, RAIN determined the peak phase for SP25°C in Figure 1F to be ZT4 ($p = 0.000015$), matching that of visual inspection and indicating a 4-hr phase delay compared to LP25°C. To test the effect of temperature, flies were reared at 25°C or 10°C in 12:12 LD cycles (Figure 1G–H). We observed a reduction in the MESOR at 10°C compared to 25°C (MESOR 25°C = 2.95, MESOR 10°C = 2.16, $p = 5x10^{-6}$; Figure 1I). Moreover, a change in the phase of the peak in PDF level was observed, with an estimated peak at ZT14 in 10°C and at ZT23 in 25°C ($p = 9x10^{-4}$; Figure 1I).

As we observed low PDF levels in simulated winter, we hypothesized that a reduction in *Pdf* mRNA could be the cause. To test this hypothesis, we conducted fluorescent *in situ* hybridization (FISH) to detect *Pdf* transcripts in brains of flies expressing *CD8::GFP* in *Pdf+* cells. We subjected these flies to either simulated summer or simulated winter. As *Pdf* mRNA expression does not show daily oscillation[53], only one timepoint (ZT16) was assessed in this experiment. A clear signal, confined to CD8::GFP positive cells, was observed (Figure 2A). This signal was absent in brains from *Pdf*-null mutants (Pdf^{01}), confirming the specificity of FISH library (Figure S1). A reduction in fluorescent signal was observed in the LNvs somas under simulated winter compared to flies reared in simulated summer (Figure 2B). Quantification of the signal from different brains show a consistent reduction in the normalized fluorescent intensity in the CD8::GFP+ cells consistent with lower levels of *Pdf* mRNA ($t(13) = 3.267$, $p = 0.0061$, Figure 2C).

Adaptation of daily locomotor activity rhythm to cold temperature and short photoperiod depends on PDF

PDF is a modulator of daily locomotor activity in *Drosophila*. Pdf^{01} mutants have previously been shown to exhibit an advancement in the evening peak of activity in LD and loss of rhythmicity under constant darkness[46]. As we observed a decrease in *Pdf* mRNA and PDF protein in simulated winter or when flies are exposed to lower temperature, we reasoned that changes in *Pdf* abundance should translate into changes in locomotor activity in response to photoperiodic and/or temperature changes, which has been shown to change over the calendar year in insects including flies. This would represent an effective readout of overall PDF abundance in flies. We therefore monitored daily activity in Pdf^{01} flies compared to Pdf^{01} mutants bearing a genomic rescue *Pdf* transgene (*yw ; Pdf{WT} ;* Pdf^{01}, hereafter denoted as genomic rescue) in selected conditions. First, flies were monitored in 12:12 LD cycles but exposed to either 25°C or 10°C. As previously described[46], Pdf^{01} flies display an advance in evening activity peak at 25°C consistent across the 5 days of monitoring. This is not observed in the genomic rescue, which has normal timing of evening peak immediately before the lights off transition at dusk (Figure 3A–B). In contrast, at 10°C, an advance in the evening peak was now observed in the genomic rescue flies and they behaved more similar to Pdf^{01} mutants (Figure 3C–D). Then, to test the effect of photoperiod, we monitored locomotor activity in short day conditions (8:16 LD) at 25°C in Pdf^{01} mutants and genomic

rescue flies. Consistent with previous studies[57], *Pdf*^{01} mutants showed a peak that is close to the lights-off transition under this condition (Figure 3E–F).

To better visualize the overall similarities of fly activity profile between the different datasets, we conducted t-distributed Stochastic Neighbor Embedding (t-SNE) analysis on the observed locomotor activity rhythms using normalized averaged daily activity profiles over 5 days (see STAR Methods for details). Overall, three distinct groups can be defined by the environmental conditions tested. While data from the genomic rescue and the *Pdf*^{01} mutants at 25°C (magenta and red dots, respectively) cluster within two broad individual groups, data between the two genotypes at 10°C (blue and yellow dots) and 8:16 (green and cyan dots) are less differentiated (Figure 3G). To further define these clustering, we used an unsupervised hierarchical clustering analysis of the normalized averaged daily activity profiles per group (see STAR Methods for calculation) (Figure 3H). Two main branches are observed, one with rescue and mutant flies at 12:12 at 25°C (black labels) and the other one containing both mutants and rescue flies at 8:16 and 10°C (red labels). These suggest that at these environmental conditions, the structure of the daily locomotor activity in mutant and rescue flies are similar to each other than to the flies at 12:12 25°C. Overall, these data suggest that temperature and photoperiod differentially modulate the evening activity in *Pdf*^{01} mutants compared to control flies.

PDF modulates overall activity level through action in *eya+* cells but its effect on timing of evening peak is not dependent on EYA

Upon release, PDF acts through activation of the G-coupled PDF receptor (PDFR)[42]. Thus, we reasoned that if PDF signaling acts through EYA to regulate changes in daily activity rhythms in response to photoperiodic and temperature changes, cells that are important in this process would coexpress *eya* and *Pdfr*. To explore this, we first used a single-cell transcriptomic (scRNA-seq) datasets available from the Fly Cell Atlas initiative[58] to determine if *Pdfr* is coexpressed with *eya* in the fly brain. Using SCOPE, a visualization tool for large sequencing dataset[59], we differentiated all cell/tissue types in the scRNA-seq dataset based on overall expression (Figure S2A), and also colored them specifically by *Pdfr* and *eya* expression (Figure S2B; green and red dots, respectively). Coexpression of both transcripts is observed in head tissue, gut, and testis cluster. Further examination showed that many of the cells expressing *eya* within the head cluster also express *Pdfr* (Figure S2B; insert).

To determine if PDF-dependent changes in daily activity rhythms in response to photoperiodic and temperature as observed in Figure 3 is mediated via EYA, we monitored locomotor activity under 12:12 LD cycles at 25°C in flies where *Pdfr* was knocked down in *eya+* cells using an *eya-Gal4* driver (Figure S3A)[24]. Interestingly, we did not observe a dramatic shift in the timing of the evening activity peak as in *Pdf*^{01} flies. This suggests that PDF signaling alters timing of evening peak through mechanisms other than EYA. We did observe, however, a decrease in the strength of the evening anticipation in *eya > Pdfr-RNAi* flies compared to controls indicated by reduced evening anticipation (Figure S3A–B). Notably the opposite is observed in flies driving a tethered version of PDF (t-PDF) using the same driver to activate PDF signaling (Figure S3C–D). This difference is even

more pronounced when looking at the overall activity level of flies in constant darkness. Knocking down *Pdfr* in *eya+* cells results in an overall reduction in total locomotion ($H(2, 86) = 17.89$, $p = 0.0001$; Figure 4A–B), while activating PDF signaling by expressing t-PDF in *eya+* cells promotes an increase in activity ($U = 333$, $p = 0.0384$; Figure 4C–D).

Previous studies have shown that PDF modulates evening anticipation by its action on non-*Pdf*-expressing clock cells within the clock network[60]. Thus, it is possible that the effect observed while knocking down *Pdfr* or expressing t-PDF in *eya+* cells is due to the modulation of these neurons. To test if *eya* is expressed in clock neurons, we detected EYA using a monoclonal antibody (Figure 4F) in flies carrying a endogenous GFP-tagged version of PER[61] to mark neurons in the clock network (Figure 4E). EYA was detected in some PER-expressing cells including DN1, LNd and DN2 neurons (Figure 4G) consistent with a role of these clusters in locomotor activity.

PDF modulates ovary size through action in *eya*+ insulin-producing cells

Expression of *eya* in the IPCs is critical for the regulation of seasonal reproductive dormancy[24]. To determine if PDF signaling works through EYA in IPCs to regulate seasonal phenotypes, we first tested if *Pdfr* is coexpressed with *eya* in these cells. Similar to a previous report[62], we observed *Pdfr*+ cells widespread across the brain (Figure S2). A cluster of cells is observed in the PI where the IPCs are located (Figure 5A, inset). We used SCOPE to plot all the cells from the dilp2IPC SMART-seq dataset, generated from isolated IPCs by fluorescence-activated cell sorting[58], and colored them by *Pdfr* and *eya* (Figure 5B; green and red dots). We observed *eya* expression in a small number of cells and some of them also express *Pdfr* (Figure 5B; yellow dots). We then detected EYA using a monoclonal antibody in *Pdfr > CD8::GFP* brains, focusing on this cluster. As previously described[24], EYA expression is observed within these cells, consistent with its expression in the IPCs, and is within the *Pdfr+* cells (Figure 5C, blue arrows). Thus, both transcriptomic and immunohistochemistry data support the notion that EYA and PDFR are coexpressed in the IPCs in fly brains.

We showed that PDF levels decrease in winter-like conditions (Figures 1–2), while our previous study showed that EYA levels increase under similar conditions. This suggests opposite functions of PDF vs EYA. To validate the antagonistic relationship between PDF and EYA, we knocked down *Pdfr* or *eya* in the IPCs and examined ovary size in summer-like conditions. We hypothesized that, knocking down *Pdfr* in this condition, should render smaller ovaries and knocking down *eya* even in summer-like condition may produce bigger, more developed ovaries, as *eya* promotes winter physiology and reproductive dormancy. As expected, knocking down *Pdfr* generated a reduction in the ovary size in summer conditions compared to the parental controls, while the same manipulation for *eya* produced the opposite effect, suggesting opposite roles of EYA and PDF in ovary development in summer-like conditions ($F(4, 173) = 177.8$, $p < 0.0001$; Figure 5D). We did not perform a parallel experiment in winter-like conditions given we have previously shown that knocking down *eya* in winter-like conditions resulted in lower levels of reproductive dormancy[24]. Moreover, we do not anticipate further reduction of ovary size if we knock down *Pdfr* in winter-like conditions when ovaries are already undeveloped with no eggs. Taken together,

these data suggest that PDF modulates ovary size through its action in *eya* expressing cells and PDF and EYA function antagonistically.

EYA protein but not mRNA is modulated by PDF

We next sought to determine if PDF could act upstream of EYA. First, we quantified *eya* mRNA in heads of Pdf^{01} and genomic rescue flies entrained in 12:12 LD cycles at 25°C. We observed no differences in *eya* abundance at all time points over the 24 hour cycle ($F(1, 56) = 0.9281$, $p = 0.3395$; Figure 6A). Nonetheless, statistical analysis of rhythmicity revealed that *eya* exhibits rhythmic expression in the genomic rescue flies (RAIN $p = 0.0078$), while it is not rhythmic in Pdf^{01} mutants (RAIN $p = 0.833$). Then, to determine if EYA protein level is different between the two genotypes, we assayed EYA abundance in protein extracts of heads from Pdf^{01} mutants or genomic rescue flies. Remarkably, we observed a dramatic increase in the overall amount of EYA protein in Pdf^{01} mutants as compared to the genomic rescue throughout the 24 hour cycle ($F(1, 55) = 50.01$, $p < 0.0001$; Figure 6B–C). Similar to our observation with *eya* mRNA, EYA protein showed daily rhythmic expression only in the genomic rescue (RAIN $p = 0.0398$), no robust daily rhythmicity was observed in Pdf^{01} mutants (RAIN $p = 0.667$).

To confirm these findings, we repeated the experiment using a control fly line in the same genetic background (*yw*) as the Pdf^{01} mutant, given that the genomic rescue might not fully recapitulate these control flies. An increase in EYA levels was still observed at ZT4 in Pdf^{01} mutants compared to control *yw* flies or the genomic rescue ($F(2, 40) = 17.92$, $p < 0.0001$; Figure 6D–E). To test if the effect of Pdf^{01} mutation in EYA protein levels is mediated by function of PDF signaling in *eya+* cells, we knocked down *Pdfr* using the *eya-Gal4* driver. Similarly to the Pdf^{01} mutant, an increase in the levels of EYA was observed in these flies ($F(2, 18) = 30.64$, $p < 0.0001$; Figure 6F–G). Conversely, expressing t-PDF to activate PDF signaling in the same *eya+* cells triggered the opposite effect; flies expressing t-PDF showed lower EYA levels than flies expressing a scrambled (SCR) peptide ($F(1, 16) = 8.268$, $p = 0.0110$; Figure 6H–I). These results suggest that PDF signaling can modulate EYA protein levels.

PKA phosphorylates EYA to modulate its stability

Because PDF negatively affected EYA protein level with no changes in overall *eya* mRNA (Figure 6), we hypothesized that PDF modulates EYA stability through post-translational modification. PDFR activation leads to increased cAMP[42,63] and subsequent activation of Protein kinase A (PKA) (Figure 7A). Interestingly, we found using pkaPS[64], a prediction tool to find PKA target sites in a given protein, that EYA contains seven potential PKA phosphorylation sites: three of them in the C-terminal, one between the second Proline-Serine-Threonine (PST) rich domain and the EYA domain (ED1), and two within the ED1 domain. To test if PKA could phosphorylate EYA, we expressed EYA alone in *Drosophila* S2 cells or together with PKA-C1, the enzymatically active subunit of this kinase[65]. We observed slower migrating EYA isoforms when EYA and PKA-C1 are coexpressed (Figure 7B). When treated with lambda phosphatase (λPP), we observed a clear mobility shift to faster migrating isoforms indicating that EYA is indeed phosphorylated by PKA-C1 in S2 cells. This data combined with the observation of EYA accumulation upon knockdown of

Pdfr (Figure 6) suggest that PKA potentially phosphorylates EYA to modulate its stability. To test this, we conducted a cycloheximide (CHX) chase experiment in S2 cells transfected with EYA alone or cotransfected with EYA and PKA-C1. CHX was added to S2 cells to inhibit translation of new proteins, thus enabling the measurement of EYA stability in the presence or absence of PKA-C1. Samples were collected at 0, 3, 6 and 9 hours after CHX application (Figure 7C). PKA expression increased EYA degradation rate, evidenced by a significant decrease in EYA levels after 3 hours of CHX addition as compared to the condition without PKA ($F(1, 24) = 7.689$, $p = 0.0106$; Figure 7C–D). Moreover, a mobility shift to higher molecular weight isoforms in EYA is clearly observed at 3, 6 and 9 hours post CHX in the presence of PKA-C1 coexpression (Figure 7C). Overall, our results suggest that PDF promotes PKA-dependent EYA phosphorylation and degradation.

DISCUSSION

The mechanisms by which organisms sense photoperiod and temperature to adapt to seasons have been studied for many years, but the core molecular components involved in this process are still unclear. In this study, we showed that the circadian neuropeptide PDF can respond to environmental cues to modulate seasonal phenotypes via EYA-dependent and independent mechanisms. Our findings suggest that PDF level is responsive to both photoperiodic and temperature changes. We proposed that under summer days, high PDF levels promote EYA degradation via PKA-dependent phosphorylation. In contrast, under winter days, a reduction in PDF drives accumulation of EYA to induce EYA-dependent changes in seasonal phenotypes, such as reproductive dormancy and changes in overall activity levels.

While other studies have explored the differences in PDF levels with environmental conditions, the results have been ambiguous[66,67]. Here we showed that during short and cold days, PDF levels are greatly reduced compared to long and warm days, effect driven by a reduction in *Pdf* mRNA levels (Figure 1–2). This is consistent with a previous observation from our lab showing *Pdf* as one of the transcripts that is downregulated in head of *Drosophila suzukii* winter morphs[68]. Overall changes in PDF can be largely explained by temperature, however, it is not clear how temperature changes results in changes in *Pdf* levels. Several factors have been found to modulate *Pdf*/PDF expression. For instance, neuronal activity and expression of CLK repress *Pdf* transcription, possibly through Hormone Receptor 38 (HR38) and stripe (SR)[39], a nuclear hormone receptor and a transcription factor, respectively. *Pdf* levels have also been shown to increase in response to high-intensity light through HR38 action[54]. In contrast, expression of VRILLE, a repressor in a secondary TTFL, promotes *Pdf/PDF* mRNA and protein accumulation in the sLNvs through a post-transcriptional mechanism[40]. Hence, it is possible that changes in core clock components are involved in the reduction in *Pdf*/PDF levels with cold temperatures. Interestingly, some core clock components are sensitive to temperature[69–72]. Alternative splicing of *per* and *tim* occurs at low temperature[69–73]. At 18°C, there is an increase in splicing of an intron located in the 3’ end of *per*, which leads to a phase advance in *per* levels, which ultimately drives a phase advance in the evening peak of locomotor activtiy[70]. We showed that at 10°C, control flies also display an advanced evening peak. This pattern resembled that of Pdf^{01} flies at 25°C, which show a similar evening peak advance (Figure 3).

Also, *Pdf*^{01} evening peak at 12:12 LD at 25°C falls close to the lights off transition similar to what it would be on a short day as shown here and in previous studies[57]. Thus, it is possible that these changes rely on a *per/Pdf* dependent pathway. At similar temperatures, an intron retention event in *tim* generates a shorter version of *tim* named *short and cold* (*tim-sc*)[72,73]. Interestingly, overexpression of *tim-sc* using a *tim-Gal4* driver generates akin but less pronounced changes in evening anticipation with flies initiating evening anticipation at around ZT7, similar to the time it starts in *Pdf*^{01} at 25°C or genomic rescue flies at 10°C[72]. We previously showed that TIM-SC protein is indeed expressed at 10°C and experiments in S2 cells showed that TIM-SC interacts with EYA to modulate its stability[24]. However, it is not known if this isoform has any impact on the function of the molecular clock, ultimately affecting PDF levels. Martin Anduaga et al.[72] showed that TIM-SC has reduced binding to PER compared to TIM-L, the canonical TIM isoform expressed at 25°C. Thus, the presence of TIM-SC during cold temperatures could potentially reduce PER stability or its translocation to the nucleus, causing CLK-CYC to promote the *Pdf* reduction through HR38 and SR.

Considering our hypothesis that PDF signaling conveys photoperiodic and temperature cues to regulate seasonality via EYA and the previously identified role of EYA in winter physiology[17,24,33], we expected that knocking down *Pdfr* or activating PDF signaling by overexpressing t-PDF in *eya+* cells would alter seasonal adaptations. These manipulations rendered different locomotor and reproductive outputs. While we were unable to reproduce the phase advance in the evening peak observed in *Pdf*^{01} flies, we observed that knocking down *Pdfr* decreased overall activity akin to a winter-like quiescent state while expressing t-PDF in the same cells rendered the opposite effect (Figure 4). This suggest that PDF modulates evening phase and overall locomotion by EYA-independent and -dependent pathways, respectively. Also in accordance with our previous results, knocking down *eya* in the IPCs results in bigger ovaries even in long and warm days[24]. Notably, this is opposite to the phenotype observed when knocking down *Pdfr*, suggesting that PDF signaling may be antagonizing EYA function. This could be possible as the IPCs receive direct inputs from the s-LNvs to modulate seasonal reproduction. Activating PDF cells increases egg laying at 25°C[74], and the same manipulation at 12°C inhibits reproductive dormancy[52]. In contrast, silencing the same neurons promotes this winter adaptation, likely through a direct effect of PDF on the IPCs. This is because *Pdfr* in the IPCs is sufficient to rescue dormancy levels in a *Pdfr* mutant[52]. Taken together, these data suggest that PDF functions in the IPCs to promote summer physiology, likely in an EYA-dependent manner.

We showed that cold temperature and short days trigger a reduction in *Pdf*/PDF mRNA and protein (Figure 1–2). Interestingly, this response is opposite of what we previously observed for EYA[24], whose expression increase in winter, and the opposite role of PDF and EYA in seasonal adaptations. Thus, we reasoned that PDF may be upstream and convey environmental signals to modulate EYA. Consistent with this, EYA levels were observed to be increased in *Pdf*^{01} mutants, also suggesting a role of PDF in inhibiting EYA expression (Figure 6). Additionally, expression of t-PDF in *eya+* cells was sufficient to decrease EYA levels, while an increase in EYA was observed when *Pdfr* was knocked down. This strongly suggests an inhibiting role of PDF on EYA. We proposed that the action of PDF signaling cascade would be involved in this. Consistent with this notion, we showed in S2 cells

that the PKA-C1, the catalytic subunit of PKA and downstream target of PDF signaling, can modulate EYA levels by phosphorylation-dependent degradation (Figure 7). PKA-C1 is also constitutively expressed in the IPCs, thus a similar process is likely happening *in vivo*[75]. Nonetheless, although PDFR signals through a cAMP/PKA[42,52], it is not the only receptor that uses this pathway to regulate seasonal biology. Indeed, dopamine and serotonin signaling in the IPCs, which also leverage cAMP/PKA, are required to promote dormancy[76]. Interestingly, this is opposite to what is observed for PDF signaling. Future studies to tease apart the contribution of PKA in the IPCs to regulate seasonal biology via EYA will require the identification and characterization of PKA-dependent EYA phosphorylation sites.

We previously showed that the interaction of TIM with EYA may be important for EYA stabilization. Interestingly, TIM is not expressed in the IPCs and EYA is not expressed in PDF-producing LNvs based on available data. These proteins seem to colocalize mainly in the optic lobes, potentially relaying seasonal cues to downstream neurons[24]. We therefore speculate TIM-EYA interaction in visual cells might be important to modulate the events in the IPCs; EYA-TIM interaction in the optic lobe could modulate the sLNvs and PDF levels downstream, consequently impacting EYA abundance and function in the IPCs to regulate seasonal physiology. Future work will be necessary to untangle the relationship between TIM and EYA in the context of the neuronal circuit.

Finally, a similar mechanism could be driving seasonal adaptations in other animals. Several studies have suggested a functional homology between the vasoactive intestinal peptide (VIP) and PDF in circadian rhythms and seasonal adaptations[77,78]. VIP is expressed by neurons located in the suprachiasmatic nucleus (SCN), the main hub for circadian timekeeping in the brain[79]. This peptide is important for circadian synchronization of the SCN individual clocks and activates the VPAC2 receptor, a class B G-protein coupled receptor that increases cAMP/PKA upon activation, similar to PDFR in *Drosophila*[77]. VIP is also indispensable for seasonal adaptations, as VIP knockout mice do not display behavioral or physiological adaptations while entrain to different photoperiods[78]. VIP is also expressed in the hypothalamus in birds and its levels are coupled to photoperiod and hormonal adaptations[80,81]. It would be interesting to explore possible modulations of EYA by VIP in the *pars tuberalis* and its effect on seasonal adaptations.

In summary, our study proposed a mechanism by which the circadian clock conveys photoperiod and temperature to clock outputs, to modulate seasonal adaptations. While we attribute the connection between the clock and the outputs to a role of a circadian neuropeptide, the molecular mechanism driving the modulation of the neuropeptide in response to environmental cues are still an open question. Furthermore, our study provides additional support for a role of EYA in seasonal adaptations and uncovers the importance of EYA post-translational modifications in the regulation of the seasonal biology.

STAR METHODS

Resource availability

Lead Contact—Further information and requests for resources and reagents should be directed to and will be fulfilled by the lead contact Joanna C. Chiu (jcchiu@ucdavis.edu).

Materials Availability

All reagents used in this study are available from the lead contact without restriction.

Data and Code Availability

- Raw data for all datasets used in this study, including microscopy, western blots, and locomotor activity data are available upon request to the lead contact. This paper also analyzes existing, publicly available data from single-cell RNA-sequencing[58]. These data are available at https://flycellatlas.org/scope.
- Single-cell RNA-sequencing data was analyzed using SCOPE, available at https://scope.aertslab.org/#/FlyCellAtlas/*/welcome. ImageJ macros used to analyze microscopy data and R code used to analyze *Drosophila* locomotor activity data will be shared upon request to the lead contact.
- Any additional information required to reanalyze the data reported in this paper is available from the lead contact upon request.

Experimental Model and Subject Details

Flies were reared on standard corn-yeast diet and kept at 25°C on a 12-hour light (L): 12-hour dark (D) cycle (12:12 LD). Fly stock were either obtained from Bloomington *Drosophila* Stock Center (BDSC), Vienna *Drosophila* Research Center (VDRC) or gifts from other labs described in the Key Resources Table.

Methods details

***Drosophila* whole-brain immunofluorescence—**Newly emerged flies were collected and placed under 12:12 LD cycles at 25°C for 3 days before switching them to long photoperiod (16:8 LD at 25°C), short photoperiod (8:16 LD at 25°C), low temperature (12:12 LD at 10°C), simulated winter (8:16 LD at 10°C), simulated summer (16:8 LD at 25°C) or kept in equinox conditions (12:12 LD at 25°C) for 7 days. Flies were collected at ZT0, 4, 8, 12, 16 and 20 hours where ZT0 represents lights on time (Zeitgeber Time; ZT), fixed for 40 minutes in 4% PFA at room temperature and dissected immediately. Brains were re-fixed in 4% PFA for 20 minutes, washed 3 times in 0.2% PBST, 15 minutes per wash, and then incubated in blocking solution (5% NGS, 0.05% Sodium Azide in 0.2% PBST) for 30 minutes. All this process was conducted at room temperature. After that, brains were incubated with primary antibody for 2 days at 4°C. Brains were then washed 3 times in 0.2% PBST, 15 minutes per wash, and then incubated at room temperature with a secondary antibody tagged with a particular fluorophore. Finally, brains were mounted using ProLong Diamond Antifade Mountant (Life Technologies, Carlsbad, CA) and imaged using a Leica SP5 confocal microscope equipped with excitation diodes at 638 nm and OPSL exciting at 488. For the experiments determining PDF levels in the s-LNvs dorsal terminals, images were taken every 1 μm using a 40x oil objective and digital zoom. For images of the whole brain, a 20x objective was used instead. All images were analyzed using Fiji and PDF levels were assessed as the intensity in the s-LNVs dorsal terminal normalized by the background signal in the same dorsal region. This process was automatized in Fiji.

The dilution of the primary antibodies is as follow: α-PDF (1:200), α-EYA (1:200), α-brp (nc82; 1:50), and α-GFP (1:1,000). The dilution of the secondary antibodies is as follow: Alexa647 α-mouse IgG (1:1,000) and Alexa488 α-chicken IgG (1:1,000).

Fluorescence *in situ* hybridization (FISH)—FISH against *Pdf* was carried out as described in Long et al.[82], with minor modifications. Flies were fixed in 4% PFA for 40 minutes and brains were dissected in cold 0.5% PBST (1X PBS, 0.5% Triton X-100) solution. Dissected brains were re-fixed in 2% PFA for 55 minutes, washed with 0.5% PBST and then dehydrated for storage with EtOH series at 30%, 50%, 70%, 100%, 100%, 100% for 10 min each. Next day, the tissue was rehydrated with inverse EtOH series 70%, 50%, 30% for 10 min each. Tissue was then washed with ice cold 1X PBS and re-fixed in 2% PFA for 55 min. After that, brains were permeated with 5% acetic acid for 5 min on ice and then washed with 0.5% PBST three times. Autofluorescence quenching was achieved by incubating the brains with 1% sodium borohydride in 3 consecutive washes for 10 min each. The tissue was primed with pre-hybridization solution (15% formamide, 2X SCC, and 0.1% Triton X-100) at 50°C for 2 hours and then hybridization was carried out in hybridization solution (10% Formamide, 2X SCC, 5X Denhard's solution, 1 mg/mL Yeast tRNA, 100 μg/mL Salmon sperm DNA, 0.1% SDS) for 10 hours at 50°C followed by 10 hours at 37°C. Probes were tagged with CAL Fluor Red 635, purchased from Biosearch Technologies (Stellaris RNA FISH probes; Petaluma, CA) (Table S1). Tissue was washed with pre-hybridization solution 3 times, 10 min each, then with 30% formamide solution supplemented with 2X SCC and 0.06% Triton X-100 twice for 30 min each. After that, tissue was washed with 2X SCC solution with 0.06% Triton three times, 10 min each, followed by a 10 min wash with 1X PBS. Finally, brain was fixed with 2% PFA for 55 minutes, washed with 0.5% PBST and then mounted ProLong Diamond Antifade Mountant (Life Technologies).

***Drosophila* Activity Monitoring (DAM) system—**Locomotor activity was measured using the DAM system (TriKinetics, MA)[83]. Flies were anesthetized under CO_2 and loaded in individual glass tubes containing fly food (5% sucrose and 2% Bacto agar in distilled water). Tubes were loaded in monitors and placed inside the incubator at 25°C under 12:12 LD cycle. After 2 days of acclimation, locomotor activity was recorded for 5 days in LD conditions and released into constant darkness (DD) for 5 days. Only flies that survived until the last day of the experiments were considered for analysis. Average locomotor activity profiles were generated for LD and DD for the 5 days in both conditions and the total locomotor activity was quantified as the sum of all the locomotor events in that given period as beam breaks per 30-min bins. The evening anticipation was calculated as the difference between the normalized averaged activity in ZT9–11.5 and ZT5–7.5 to understand the strength/amplitude of the peak.

For clustering analysis, we transformed the raw *Drosophila* activity monitoring data into a 24-hour activity matrix that describes the normalized activity profile of each fly as follows. The average beam breaks (or activity counts) per 30 mins from ZT0 to ZT24 was obtained across 5 days to compute an average activity profile per fly composed of 48 values (1 value per 30-min bin). Each of those 48 values was then divided by the value of the

bin with the highest activity count such that the bin with the highest value equals to 1. We chose to perform this normalization step to focus on the 24h activity profile without taking into account the differences in absolute activity level. These 48 values are now used as a descriptor for the flies' activity profiles and analyzed using t-distributed Stochastic Neighbor Embedding (t-SNE). t-SNE was calculated using the "Rtsne" package[84] on R, using perplexity 30, max iterations 1000 and 50 initial dimensions. Each dot represents the first two dimensions of the 48 values now reduced for each fly. t-SNE was used to mathematically transform high-dimensional data (48 values per fly) and project it into low-dimensional space[85]. The two dimensions on the t-SNE plot do not represent specific parameters. They hold no meaning on their own, unlike axes of conventional 2D graphs. The information gathered by this analysis is qualitative and is used to extrapolate the similarity of daily fly activity rhythms as visual clustering in a 2D space, i.e. data points that are closer to each other represent flies with more similar daily activity patterns.

Hierarchical clustering also used this 48 starting values per fly and the analysis was conducted using the "stat" package on R[86]. First, a distance matrix was created using "dist" function, using the "maximum" method. Then, clustering was conducted using "hclust" function using "ward.D" method. Finally, a dendrogram was generated using "as.dendrogram" function and plotted using the "plot" function from the "base" package.

Ovary size quantification—Virgin females were placed in simulated summer conditions (25°C, 16:8 LD) for 28 days and then dissected in 0.2% PBST (0.2% Triton X-100 in 1X PBS)[24]. Ovaries were imaged using a EVOS microscope (Life Technologies, CA) and ovary size was determined by measuring the surface area (mm^2) using Fiji software.

Total RNA extraction and quantitative RT-PCR—Flies were collected at the indicated timepoints on dry ice and then heads were collected and stored at −80°C until sample processing. Around 20-50 μL of heads per condition were processed using TRI reagent (Sigma-Aldrich, St. Louis, MO), following manufacturer's instructions. Total RNA was quantified and 1 μg was used as starting material for reverse transcription using the Superscript IV cDNA synthesis kit (Life Technologies) following manufacturer's instruction. Quantitative PCR was performed using SsoAdvanced Universal SYBR green super mix (Bio Rad, Hercules, CA), with the following the program: initial 95°C for 30 seconds, then 40 cycles of 95°C for 5 seconds, followed by an annealing/extension phase at 60°C for 30 seconds. Primers to detect *eya* were 5'-GAGGCCTGGCTACAGATACG-3' and 5'-AGTTGCGTGGAGGTTACCAG-3', while *cbp20* (5'-GTCTGATTCGTGTGGACTGG-3' and 5'-CAACAGTTTGCCATAACCCC-3') was used for normalization. Data were analyzed using the ΔΔCt method.

Protein extraction from heads and western blotting—Protein extraction from fly heads was conducted as previously described[24,87–89]. Flies were collected at the indicated timepoints and flash frozen using dry ice. Heads were then collected and ground on protein extraction buffer (0.1% Glycerol, 20mM Hepes pH7.5, 50mM KCl, 2mM EDTA, 1% Triton X-100, 0.40% NP 40, 1mM DTT, 10μg/mL Aprotinin, 5μg/mL Leupeptin, 1μ/mL Pepstatin A and 0.5mM PMSF). Protein samples were kept at −80°C in SDS loading buffer until electrophoresis in 8% SDS-PAGE gels. Transfer was conducted in a Trans-Blot semi-dry

transfer system (Bio Rad) for 45 minutes to nitrocellulose membranes (0.45μm, Bio Rad). 5% blocking reagent (Bio Rad) in 0.05% TBST (0.05% Tween20 in 1XTBS) was used to block for 1 hour before antibody incubation overnight at 4°C. Anti-mouse IgG linked to HRP (Cytiva Life Sciences, Malborough, MA) was used as a secondary antibody at a dilution of 1:1,000 incubated for 1 hour. Membranes were incubated for 5 min with Clarity reagent (Bio Rad) and imaged on ChemiDoc MP Imaging system. Image analysis was performed using Image J. The dilution of the primary antibodies is as follow: μ-EYA (1:1,000), μ-HSP70 (1:7,000), μ-V5 (1:5,000), and μ-FLAG (1:7,000).

Drosophila* S2 cell culture and transfection—Drosophila* S2 cells were maintained at 22°C in Schneider's *Drosophila* medium (Life Technologies) supplemented with 10% Fetal Bovine Serum (VWR, Radnor, PA). For both cycloheximide (CHX) chase and phosphatase experiments, on day one, 3×10^6 cells were transiently transfected with 0.8 μg *pAc-eya-3XFLAG-6XHis* and 0.2 μg *pMT-PKA-C1-V5* or an empty *pMT-V5* plasmid. PKA-C1 expression was induced 24 hours after transfection by addition of 500 μM $CuSO_4$.

λ Phosphatase experiments—For phosphatase treatment, cells were treated with cycloheximide (CHX) for 3 hours to a final concentration of 10 μg/ml. Cells were harvested and proteins were extracted using EB2 (20 mM HEPES pH 7.5, 100 mM KCl, 5% glycerol, 5 mM EDTA, 1 mM DTT, 0.1% Triton X-100, 10 μg/ml Aprotinin, 5 μg/ml Leupeptin, 1 μg/ml Pepstatin A, 0.5 mM PMSF, 25 mM NaF)[88] supplemented with 1X PhosSTOP (Roche, Indianapolis, IN).

Protein quantification was carried out using Coomassie reagent and the same amount of protein was aliquoted for PKA+ and PKA- conditions. α-FLAG immunoprecipitation was performed using anti-FLAG M2 agarose (Sigma) following protocol described in Lam et al.[88]. Beads were incubated with the protein lystes in and end-to-end rotator for 4 hours at 4°C. Immunocomplexes were then treated with Lambda phosphatase λ-PP or mock treated (New England Biolabs, Ipswich, MA) for 30 min at 30°C in a water bath, flicking the tube every 10 min. Finally, the beads were precipitated, and the proteins were obtained by adding 2x SDS sample buffer and then resolved in 8% SDS-PAGE.

Cycloheximide experiments—For CHX chase assay to measure protein degradation, CHX was added to the transfected cells, again at 24 hours after kinase induction to a final concentration of 10 μg/ml. S2 cells were harvested immediately, or at 3, 6, 9 hours after addition of CHX. Upon cell harvest, proteins were extracted using EB2 and resolved in 8% SDS-PAGE.

Quantification and statistical analysis—Data are represented as mean ± standard error of the mean (SEM) in XY graphs. For all other representations, whiskers and boxes were used, and the result of each biological replicate is represented in the graphs as a single dot. Circadian analysis was conducted using the R package CircaCompare[55] or RAIN[56] as indicated in each figure. All datasets were assessed for normality using a Shapiro-Wilk's normality test to choose the appropriate parametric or non-parametric test. Tests used for each dataset are indicated in figure legends. Statistical differences reported throughout this

work are ns $p > 0.05$, * $p < 0.05$, ** $p < 0.01$, *** $p < 0.001$ and **** $p < 0.0001$. The number of biological replicates is indicated in each figure or figure legend.

Supplementary Material

Refer to Web version on PubMed Central for supplementary material.

ACKNOWLEDGEMENTS

We would like to thank all the members of the Chiu lab and Hamada lab for providing valuable comments in the development of the project. We also want to thank Dr. Yong Zhang for the PER-AID-GFP fly line and Dr. Pamela Ronald for access to the confocal microscope (Leica SP8 from NIH grant GM122968). S.H. is a Latin American Fellow in the Biomedical Sciences supported by the Pew Charitable Trusts. Research in the lab of JCC is supported by NIH R01 DK124068. Graphical abstract was generated on Biorender (license to UC Davis Chiu lab).

REFERENCES

1. Stevenson TJ, Prendergast BJ, and Nelson RJ (2017). Mammalian Seasonal Rhythms: Behavior and Neuroendocrine Substrates. In Hormones, Brain and Behavior: Third edition (Academic Press), pp. 371–398. 10.1016/B978-0-12-803592-4.00013-4.
2. Nelson R, (1990). Mechanisms Of Seasonal Cycles Of Behavior. Annu. Rev. Psychol 41, 81–108. 10.1146/annurev.psych.41.1.81. [PubMed: 2407180]
3. Alerstam T, and Bäckman J, (2018). Ecology of animal migration. Curr. Biol 28, R968–R972. 10.1016/J.CUB.2018.04.043. [PubMed: 30205072]
4. Chowdhury S, Fuller RA, Dingle H, Chapman JW, and Zalucki MP, (2021). Migration in butterflies: a global overview. Biol. Rev 96, 1462–1483. 10.1111/brv.12714. [PubMed: 33783119]
5. Ray S, Li M, Koch SP, Mueller S, Boehm-Sturm P, Wang H, Brecht M, and Naumann RK, (2020). Seasonal plasticity in the adult somatosensory cortex. Proc. Natl. Acad. Sci. U. S. A 117, 32136–32144. 10.1073/pnas.l922888117. [PubMed: 33257560]
6. Liu W, Feke A, Leung CC, Tarté DA, Yuan W, Vanderwall M, Sager G, Wu X, Schear A, Clark DA, et al. (2021). A metabolic daylength measurement system mediates winter photoperiodism in plants. Dev. Cell 56, 2501–2515.e5. 10.1016/j.devcel.2021.07.016. [PubMed: 34407427]
7. Cubas P, (2020). Plant Seasonal Growth: How Perennial Plants Sense That Winter Is Coming. Curr. Biol 30, R21–R23. 10.1016/j.cub.2019.11.044. [PubMed: 31910371]
8. Nelson RJ, (2004). Seasonal immune function and sickness responses. Trends Immunol. 25, 187–192. 10.1016/j.it.2004.02.001. [PubMed: 15039045]
9. Webb AJS, Brain SAE, Wood R, Rinaldi S, and Turner MR, (2015). Seasonal variation in Guillain-Barré syndrome: a systematic review, meta-analysis and Oxfordshire cohort study. J. Neurol. Neurosurg. Psychiatry 86,1196–1201. 10.1136/jnnp-2014-309056. [PubMed: 25540247]
10. Tendler A, Bar A, Mendelsohn-Cohen N, Karin O, Kohanim YK, Maimon L, Milo T, Raz M, Mayo A, Tanay A, et al. (2021). Hormone seasonality in medical records suggests circannual endocrine circuits. Proc. Natl. Acad. Sci. U. S. A 118. 10.1073/pnas.2003926118.
11. Sun L, Tang J, Liljenbäck H, Honkaniemi A, Virta J, Isojärvi J, Karjalainen T, Kantonen T, Nuutila P, Hietala J, et al. (2021). Seasonal variation in the brain μ-opioid receptor availability. J. Neurosci 41, 1265–1273. 10.1523/JNEUROSCI.2380-20.2020. [PubMed: 33361461]
12. Hand SC, Denlinger DL, Podrabsky JE, and Roy R, (2016). Mechanisms of animal diapause: Recent developments from nematodes, crustaceans, insects, and fish. Am. J. Physiol. - Regul. Integr. Comp. Physiol 310, R1193–R1211. 10.1152/ajpregu.00250.2015. [PubMed: 27053646]
13. Hazlerigg DG, and Wagner GC, (2006). Seasonal photoperiodism in vertebrates: from coincidence to amplitude. Trends Endocrinol. Metab 17, 83–91. 10.1016/j.tem.2006.02.004. [PubMed: 16513363]
14. Anduaga AM, Nagy D, Costa R, and Kyriacou CP (2018). Diapause in *Drosophila melanogaster*- Photoperiodicity, cold tolerance and metabolites. J. Insect Physiol 105, 46–53.10.1016/j.jinsphys.2018.01.003. [PubMed: 29339232]

15. Nakayama T, and Yoshimura T, (2018). Seasonal Rhythms: The Role of Thyrotropin and Thyroid Hormones. Thyroid 28, 4–10.10.1089/thy.2017.0186. [PubMed: 28874095]
16. Ikegami K, Refetoff S, Van Cauter E, and Yoshimura T, (2019). Interconnection between circadian clocks and thyroid function. Nat. Rev. Endocrinol 15, 590–600. 10.1038/s41574-019-0237-z. [PubMed: 31406343]
17. Nakao N, Ono H, Yamamura T, Anraku T, Takagi T, Higashi K, Yasuo S, Katou Y, Kageyama S, Uno Y, et al. (2008). Thyrotrophin in the pars tuberalis triggers photoperiodic response. Nature 452, 317–322. 10.1038/nature06738. [PubMed: 18354476]
18. Hazlerigg D, Lomet D, Lincoln G, and Dardente H, (2018). Neuroendocrine correlates of the critical day length response in the Soay sheep. J. Neuroendocrinol 30, el2631. 10.1111/jne.12631.
19. Schiesari L, Kyriacou CP, and Costa R, (2011). The hormonal and circadian basis for insect photoperiodic timing. FEBS Lett. 585,1450–1460. 10.1016/j.febslet.2011.02.026. [PubMed: 21354417]
20. Xu WH, Lu YX, and Denlinger DL, (2012). Cross-talk between the fat body and brain regulates insect developmental arrest. Proc. Natl. Acad. Sci. U. S. A 109, 14687–14692. 10.1073/pnas.1212879109. [PubMed: 22912402]
21. Denlinger DL, Hahn DA, Merlin C, Holzapfel CM, and Bradshaw WE, (2017). Keeping time without a spine: What can the insect clock teach us about seasonal adaptation? Philos. Trans. R. Soc. B Biol. Sci 372.10.1098/rstb.2016.0257.
22. Kurogi Y, Mizuno Y, Imura E, and Niwa R, (2021). Neuroendocrine Regulation of Reproductive Dormancy in the Fruit Fly *Drosophila melanogaster*: A Review of Juvenile Hormone-Dependent Regulation. Front. Ecol. Evol 9, 1–16. 10.3389/fevo.2021.715029.
23. Dardente H, Wyse CA, Birnie MJ, Dupré SM, Loudon ASI, Lincoln GA, and Hazlerigg DG, (2010). A Molecular Switch for Photoperiod Responsiveness in Mammals. Curr. Biol 20, 2193–2198. 10.1016/j.cub.2010.10.048. [PubMed: 21129971]
24. Abrieux A, Xue Y, Cai Y, Lewald KM, Nguyen HN, Zhang Y, and Chiu JC, (2020). EYES ABSENT and TIMELESS integrate photoperiodic and temperature cues to regulate seasonal physiology in *Drosophila*. Proc. Natl. Acad. Sci 117,15293–15304. 10.1073/pnas.2004262117. [PubMed: 32541062]
25. Bünning E, (1936). Die endogene Tagesrhythmik als Grundlage der photoperiodischen Reaktion. Berichte Dtsch. Bot. Gessellschaft
26. Bunning E, (1960). Circadian Rhythms and the Time Measurement in Photoperiodism. Cold Spring Harb. Symp. Quant. Biol 25, 249–256. 10.1101/SQB.1960.025.01.026.
27. Patke A, Young MW, and Axelrod S, (2020). Molecular mechanisms and physiological importance of circadian rhythms. Nat. Rev. Mol. Cell Biol 21, 67–84. 10.1038/s41580-019-0179-2. [PubMed: 31768006]
28. Pittendrigh CS, and Minis DH, (1964). The Entrainment of Circadian Oscillations by Light and Their Role as Photoperiodic Clocks. Am. Nat 98, 261–294.
29. Ikeno T, Tanaka SI, Numata H, and Goto SG (2010). Photoperiodic diapause under the control of circadian clock genes in an insect. BMC Biol. 8, 116. 10.1186/1741-7007-8-116. [PubMed: 20815865]
30. Sandrelli F, Tauber E, Pegoraro M, Mazzotta G, Cisotto P, Landskron J, Stanewsky R, Piccin A, Rosato E, Zordan M, et al. (2007). A Molecular Basis for Natural Selection at the *timeless* Locus in *Drosophila melanogaster*. Science 316,1898–1900. 10.1126/science.1138426. [PubMed: 17600216]
31. Tauber E, Zordan M, Sandrelli F, Pegoraro M, Osterwalder N, Breda C, Daga A, Selmin A, Monger K, Benna C, et al. (2007). Natural Selection Favors a Newly Derived timeless Allele in *Drosophila melanogaster*. Science 316, 1895–1898. 10.1126/science.1138412. [PubMed: 17600215]
32. Pegoraro M, Gesto JS, Kyriacou CP, and Tauber E, (2014). Role for Circadian Clock Genes in Seasonal Timing: Testing the Bünning Hypothesis. PLoS Genet. 10. 10.1371/journal.pgen.1004603.

33. Wood SH, Hindle MM, Mizoro Y, Cheng Y, Saer BRCC, Miedzinska K, Christian HC, Begley N, McNeilly J, McNeilly AS, et al. (2020). Circadian clock mechanism driving mammalian photoperiodism. Nat. Commun 11, 4291. 10.1038/s41467-020-18061-z. [PubMed: 32855407]
34. Barber AF, Erion R, Holmes TC, and Sehgal A (2016). Circadian and feED1ng cues integrate to drive rhythms of physiology in *Drosophila* insulin-producing cells. Genes Dev. 30, 2596–2606. 10.1101/gad.288258.116. [PubMed: 27979876]
35. Cavanaugh DJ, Geratowski JD, Wooltorton JRA, Spaethling JM, Hector CE, Zheng X, Johnson EC, Eberwine JH, and Sehgal A (2014). Identification of a circadian output circuit for rest:activity rhythms in *Drosophila*. Cell 157, 689–701. 10.1016/j.cell.2014.02.024. [PubMed: 24766812]
36. Barber AF, Fong SY, Kolesnik A, Fetchko M, and Sehgal A, (2021). *Drosophila* clock cells use multiple mechanisms to transmit time-of-day signals in the brain. Proc. Natl. Acad. Sci. U. S. A 118, 1–8. 10.1073/pnas.2019826118.
37. Reinhard N, Bertolini E, Saito A, Sekiguchi M, Yoshii T, Rieger D, and Helfrich-Förster C, (2022). The lateral posterior clock neurons of *Drosophila melanogaster* express three neuropeptides and have multiple connections within the circadian clock network and beyond. J. Comp. Neurol 530, 1507–1529. 10.1002/cne.25294. [PubMed: 34961936]
38. Reinhard N, Schubert FK, Bertolini E, Hagedorn N, Manoli G, Sekiguchi M, Yoshii T, Rieger D, and Helfrich-Förster C, (2022). The Neuronal Circuit of the Dorsal Circadian Clock Neurons in *Drosophila melanogaster*. Front. Physiol 13, 1–29. 10.3389/fphys.2022.886432.
39. Mezan S, Feuz JD, Deplancke B, and Kadener S, (2016). PDF Signaling Is an Integral Part of the *Drosophila* Circadian Molecular Oscillator. Cell Rep. 17, 708–719. 10.1016/j.celrep.2016.09.048. [PubMed: 27732848]
40. Gunawardhana KL, and Hardin PE, (2017). VRILLE Controls PDF Neuropeptide Accumulation and Arborization Rhythms in Small Ventrolateral Neurons to Drive Rhythmic Behavior in *Drosophila*. Curr. Biol 27, 3442–3453e4. 10.1016/j.cub.2017.10.010. [PubMed: 29103936]
41. Taghert PH, and Shafer OT, (2006). Mechanisms of clock output in the *Drosophila* circadian pacemaker system. J. Biol. Rhythms 21, 445–457. 10.1177/0748730406293910. [PubMed: 17107935]
42. Shafer OT, Kim DJ, Dunbar-Yaffe R, Nikolaev VO, Lohse MJ, and Taghert PH, (2008). Widespread Receptivity to Neuropeptide PDF throughout the Neuronal Circadian Clock Network of *Drosophila* Revealed by Real-Time Cyclic AMP Imaging. Neuron 58, 223–237. 10.1016/j.neuron.2008.02.018. [PubMed: 18439407]
43. Lin Y, Stormo GD, and Taghert PH, (2004). The neuropeptide pigment-dispersing factor coordinates pacemaker interactions in the *Drosophila* circadian system. J. Neurosci 24, 7951–7957. 10.1523/JNEUROSCI.2370-04.2004. [PubMed: 15356209]
44. Helfrich-Förster C, (1998). Robust circadian rhythmicity of *Drosophila melanogaster* requires the presence of lateral neurons: A brain-behavioral study of disconnected mutants. J. Comp. Physiol. - Sens. Neural Behav. Physiol 182, 435–453. 10.1007/s003590050192.
45. Nitabach MN, Blau J, and Holmes TC, (2002). Electrical Silencing of *Drosophila* Pacemaker Neurons Stops the Free-Running Circadian Clock An important area of circadian rhythm research is the relationship between the function of the molecular clock in pacemaker neurons and the central physiological. Cell 109, 485–495. [PubMed: 12086605]
46. Renn SCP, Park JH, Rosbash M, Hall JC, and Taghert PH (1999). A pdf neuropeptide gene mutation and ablation of PDF neurons each cause severe abnormalities of behavioral circadian rhythms in *Drosophila*. Cell 99, 791–802. 10.1016/S0092-8674(00)81676-1. [PubMed: 10619432]
47. Seluzicki A, Flourakis M, Kula-Eversole E, Zhang L, Kilman V, and Allada R, (2014). Dual PDF Signaling Pathways Reset Clocks Via TIMELESS and Acutely Excite Target Neurons to Control Circadian Behavior. PLoS Biol. 12, 19–25. 10.1371/journal.pbio.1001810.
48. Shiga S, and Numata H, (2009). Roles of PER immunoreactive neurons in circadian rhythms and photoperiodism in the blow fly, *Protophormia terraenovae*. J. Exp. Biol 212, 867–877. 10.1242/jeb.027003. [PubMed: 19252004]
49. Ikeno T, Numata H, Goto SG, and Shiga S, (2014). Involvement of the brain region containing pigment-dispersing factor-immunoreactive neurons in the photoperiodic response of the bean bug, *Riptortus pedestris*. J. Exp. Biol 217, 453–462. 10.1242/jeb.091801. [PubMed: 24198258]

50. Hasebe M, Kotaki T, and Shiga S, (2022). Pigment-dispersing factor is involved in photoperiodic control of reproduction in the brown-winged green bug, *Plautia stali*. J. Insect Physiol 137, 104359. 10.1016/j.jinsphys.2022.104359. [PubMed: 35041845]
51. Ojima N, Hara Y, Ito H, and Yamamoto D, (2018). Genetic dissection of stress-induced reproductive arrest in *Drosophila melanogaster* females. PLoS Genet. 14, 1–15. 10.1371/journal.pgen.1007434.
52. Nagy D, Cusumano P, Andreatta G, Anduaga AM, Hermann-Luibl C, Reinhard N, Gesto J, Wegener C, Mazzotta G, Rosato E, et al. (2019). Peptidergic signaling from clock neurons regulates reproductive dormancy in *Drosophila melanogaster*. PLoS Genet. 15, 1–25. 10.1371/journal.pgen.1008158.
53. Park JH, Helfrich-Förster C, Lee G, Liu L, Rosbash M, and Hall JC, (2000). Differential regulation of circadian pacemaker output by separate clock genes in *Drosophila*. Proc. Natl. Acad. Sci 97, 3608–3613. 10.1073/pnas.070036197. [PubMed: 10725392]
54. Chatterjee A, Lamaze A, De J, Mena W, Chélot E, Martin B, Hardin P, Kadener S, Emery P, and Rouyer F, (2018). Reconfiguration of a Multi-oscillator Network by Light in the *Drosophila* Circadian Clock. Curr. Biol 28, 2007–2017.e4. 10.1016/j.cub.2018.04.064. [PubMed: 29910074]
55. Parsons R, Parsons R, Garner N, Oster H, and Rawashdeh O, (2020). CircaCompare: a method to estimate and statistically support differences in mesor, amplitude and phase, between circadian rhythms. Bioinformatics 36, 1208–1212. 10.1093/bioinformatics/btz730. [PubMed: 31588519]
56. Thaben PF, and Westermark PO, (2014). Detecting Rhythms in Time Series with RAIN. J. Biol. Rhythms 29, 391–400. 10.1177/0748730414553029. [PubMed: 25326247]
57. Yoshii T, Wülbeck C, Sehadova H, Veleri S, Bichler D, Stanewsky R, and Helfrich- Förster C, (2009). The neuropeptide pigment-dispersing factor adjusts period and phase of *Drosophila*'s clock. J. Neurosci 29, 2597–2610. 10.1523/JNEUROSCI.5439-08.2009. [PubMed: 19244536]
58. Li H, Janssens J, de Waegeneer M, Kolluru SS, Davie K, Gardeux V, Saelens W, David FPA, Brbić M, Spanier K, et al. (2022). Fly Cell Atlas: A single-nucleus transcriptomic atlas of the adult fruit fly. Science 375. 10.1126/science.abk2432.
59. Davie K, Janssens J, Koldere D, De Waegeneer M, Pech U, Kreft Ł, Aibar S, Makhzami S, Christiaens V, Bravo González-Blas C, et al. (2018). A Single-Cell Transcriptome Atlas of the Aging *Drosophila* Brain. Cell 174, 982–998e20. 10.1016/j.cell.2018.05.057. [PubMed: 29909982]
60. Lear BC, Zhang L, and Allada R, (2009). The neuropeptide PDF acts directly on evening pacemaker neurons to regulate multiple features of circadian behavior. PLoS Biol. 7. 10.1371/journal.pbio.1000154.
61. Chen W, Werdann M, and Zhang Y, (2018). The auxin-inducible degradation system enables conditional PERIOD protein depletion in the nervous system of *Drosophila melanogaster*. FEBS J. 285, 4378–4393.10.1111/febs.l4677. [PubMed: 30321477]
62. Im SH, and Taghert PH, (2010). PDF receptor expression reveals direct interactions between circadian oscillators in *Drosophila*. J. Comp. Neurol 518,1925–1945. 10.1002/cne.22311. [PubMed: 20394051]
63. Hyun S, Lee Y, Hong ST, Bang S, Paik D, Kang J, Shin J, Lee J, Jeon K, Hwang S, et al. (2005). *Drosophila* GPCR han is a receptor for the circadian clock neuropeptide PDF. Neuron 48, 267–278. 10.1016/j.neuron.2005.08.025. [PubMed: 16242407]
64. Neuberger G, Schneider G, and Eisenhaber F, (2007). pkaPS: prediction of protein kinase A phosphorylation sites with the simplified kinase-substrate binding model. Biol. Direct 2. 10.1186/1745-6150-2-1.
65. Søberg K, and Skålhegg BS, (2018). The molecular basis for specificity at the level of the protein kinase a catalytic subunit. Front. Endocrinol 9, 538. 10.3389/FENDO.2018.00538/BIBTEX.
66. Meiselman MR, Alpert MH, Cui X, Shea J, Gregg I, Gallio M, and Yapici N, (2022). Recovery from cold-induced reproductive dormancy is regulated by temperature-dependent AstC signaling. Curr. Biol 32, 1362–1375e8. 10.1016/j.cub.2022.01.061. [PubMed: 35176227]
67. Liao S, Broughton S, and Nässel DR, (2017). Behavioral senescence and aging-related changes in motor neurons and brain neuromodulator levels are ameliorated by lifespan-extending reproductive dormancy in *Drosophila*. Front. Cell. Neurosci 11, 1–20. 10.3389/fncel.2017.00111. [PubMed: 28154525]

68. Shearer PW, West JD, Walton VM, Brown PH, Svetec N, and Chiu JC (2016). Seasonal cues induce phenotypic plasticity of *Drosophila suzukii* to enhance winter survival. BMC Ecol. 16, 11. 10.1186/sl2898-016-0070-3. [PubMed: 27001084]
69. Chen WF, Low KH, Lim C, and Edery I, (2007). Thermosensitive splicing of a clock gene and seasonal adaptation. Cold Spring Harb. Symp. Quant. Biol 72, 599–606. 10.1101/sqb.2007.72.021. [PubMed: 18419319]
70. Majercak J, Sidote D, Hardin PE, and Edery I, (1999). How a circadian clock adapts to seasonal decreases in temperature and day length. Neuron 24, 219–230. 10.1016/S0896-6273(00)80834-X. [PubMed: 10677039]
71. Montelli S, Mazzotta G, Vanin S, Caccin L, Corrà S, De Pittà C, Boothroyd C, Green EW, Kyriacou CP, and Costa R, (2015). Period and timeless mRNA Splicing Profiles under Natural Conditions in *Drosophila melanogaster*. J. Biol. Rhythms 30, 217–227. 10.1177/0748730415583575. [PubMed: 25994101]
72. Anduaga AM, Evanta N, Patop IL, Bartok O, Weiss R, and Kadener S, (2019). Thermosensitive alternative splicing senses and mediates temperature adaptation in *Drosophila*. eLife 8, 1–31.10.7554/eLife.44642.
73. Foley LE, Ling J, Joshi R, Evantal N, Kadener S, and Emery P, (2019). *Drosophila* PSI controls circadian period and the phase of circadian behavior under temperature cycle via tim splicing. eLife 8, 1–28. 10.7554/eLife.50063.
74. Zhang C, Daubnerova I, Jang YH, Kondo S, Žitnan D, and Kim YJ, (2021). The neuropeptide allatostatin C from clock-associated DN1p neurons generates the circadian rhythm for oogenesis. Proc. Natl. Acad. Sci. U. S. A 118. 10.1073/pnas.2016878118.
75. Machado Almeida P, Lago Solis B, Stickley L, Feidler A, and Nagoshi E, (2021). Neurofibromin 1 in mushroom body neurons mediates circadian wake drive through activating cAMP-PKA signaling. Nat. Commun 12, 1–17. 10.1038/s41467-021-26031-2. [PubMed: 33397941]
76. Andreatta G, Kyriacou CP, Flatt T, and Costa R, (2018). Aminergic Signaling Controls Ovarian Dormancy in Drosophila. Sci. Rep 8, 1–14. 10.1038/s41598-018-20407-z. [PubMed: 29311619]
77. Vosko AM, Schroeder A, Loh DH, and Colwell CS (2007). Vasoactive Intestinal Peptide and the Mammalian Circadian System. Gen. Comp. Endocrinol 152, 165–175. 10.1016/j.ygcen.2007.04.018. [PubMed: 17572414]
78. Lucassen EA, van Diepen HC, Houben T, Michel S, Colwell CS, and Meijer JH, (2012). Role of vasoactive intestinal peptide in seasonal encoding by the suprachiasmatic nucleus clock. Eur. J. Neurosci 35, 1466–1474. 10.1111/j.l460-9568.2012.08054.x. [PubMed: 22512278]
79. Aton SJ, Colwell CS, Harmar AJ, Waschek J, and Herzog ED, (2005). Vasoactive intestinal polypeptide mediates circadian rhythmicity and synchrony in mammalian clock neurons. Nat. Neurosci 8, 476–483. 10.1038/nnl419. [PubMed: 15750589]
80. Yasuo S, Watanabe M, Tsukada A, Takagi T, ligo M, Shimada K, Ebihara S, and Yoshimura T, (2004). Photoinducible Phase-Specific Light Induction of Cry1 Gene in the Pars Tuberalis of Japanese Quail. Endocrinology 145, 1612–1616. 10.1210/en.2003-1285. [PubMed: 14684603]
81. el Halawani ME, Pitts GR, Sun S, Silsby JL, and Sivanandan V, (1996). Active immunization against vasoactive intestinal peptide prevents photo-induced prolactin secretion in turkeys. Gen. Comp. Endocrinol 104, 76–83. 10.1006/gcen.1996.0143. [PubMed: 8921358]
82. Long X, Colonell J, Wong AM, Singer RH, and Lionnet T, (2017). Quantitative mRNA imaging throughout the entire *Drosophila* brain. Nat. Methods 14, 703–706. 10.1038/nmeth.4309. [PubMed: 28581495]
83. Chiu JC, Low KH, Pike DH, Yildirim E, and Edery I, (2010). Assaying locomotor activity to study circadian rhythms and sleep parameters in *Drosophila*. J. Vis. Exp 10.3791/2157.
84. Krijthe JH, (2015). Rtsne: T-Distributed Stochastic Neighbor Embedding using Barnes-Hut Implementation.
85. Maaten L. van der, and Hinton G, (2008). Visualizing Data using t-SNE. J. Mach. Learn. Res 9, 2579–2605.
86. R Core Team (2020). R: A Language and Environment for Statistical Computing (R Foundation for Statistical Computing).

87. Chiu JC, Vanselow JT, Kramer A, and Edery I, (2008). The phospho-occupancy of an atypical SLIMB-binding site on PERIOD that is phosphorylated by DOUBLETIME controls the pace of the clock. Genes Dev. 22, 1758–1772. 10.1101/gad.1682708. [PubMed: 18593878]

88. Lam VH, Li YH, Liu X, Murphy KA, Diehl JS, Kwok RS, and Chiu JC, (2018). CK1α collaborates with DOUBLETIME to regulate PERIOD function in the *Drosophila* circadian clock. J. Neurosci 38, 10631–10643. 10.1523/JNEUROSCI.0871-18.2018. [PubMed: 30373768]

89. Cai YD, Xue Y, Truong CC, Del Carmen-Li J, Ochoa C, Vanselow JT, Murphy KA, Li YH, Liu X, Kunimoto BL, et al. (2020). CK2 Inhibits TIMELESS Nuclear Export and Modulates CLOCK Transcriptional Activity to Regulate Circadian Rhythms. Curr. Biol 10.1016/j.cub.2020.10.061.

Highlights

- PDF level is sensitive to temperature and photoperiod.
- PDF modulates seasonal biology through EYA-dependent and independent mechanisms.
- EYA protein level is regulated by PDF signaling pathway.
- EYA is phosphorylated by Protein Kinase A to promote its degradation.

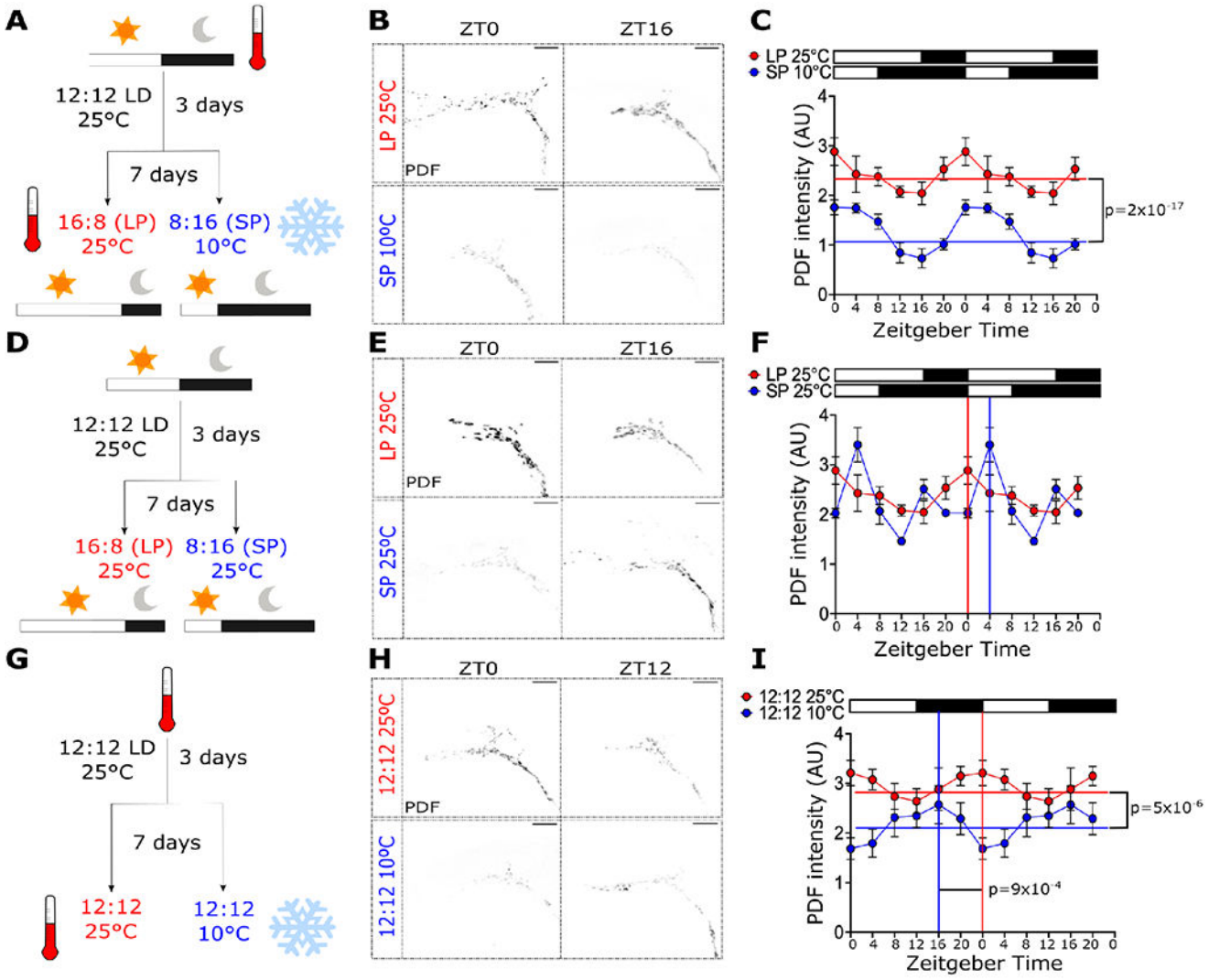

Figure 1. PDF levels are regulated by photoperiod and temperature.

PDF levels in the s-LNv dorsal terminals were analyzed in flies entrained to (A) long-photoperiod (LP, 16:8 LD) at 25°C or short-photoperiod (SP, 8:16 LD) at 10°C, (D) LP or SP at 25°C, and (G) 12:12 LD cycles at 25°C or 10°C. Representative images for these conditions at ZT0 and ZT16 or ZT12 are shown in B, E and H, respectively. Double-plotted graphs of PDF signal for each condition are shown in C, F and I, respectively. White boxes represent lights-on, and black boxes represent lights-off. CircaCompare and RAIN was used to determine rhythmicity and phase for all datasets. MESOR (horizontal lines) and phase (vertical lines) are displayed in the graphs if statistically significant ($p < 0.05$), except for (F), where the phases detected between CircaCompare and RAIN were different. The phases shown in (F) were calculated using RAIN. Scale bars are 10 μm. Number of brains imaged were LP25: ZT0 n = 18, ZT4 n = 11, ZT8 n = 13, ZT12 n = 18, ZT16 = 9, ZT20 n = 14; SP10: ZT0 n = 9, ZT4 n = 8, ZT8 n = 14, ZT12 n = 14, ZT16 = 18, ZT20 n = 20; SP25 ZT0 n = 6, ZT4 n = 8, ZT8 n = 9, ZT12 n = 6, ZT16 =10, ZT20 n = 3; 12:12 25°C: ZT0 n = 14,

ZT4 n = 14, ZT8 n = 15, ZT12 n = 19, ZT16 =10, ZT20 n = 15; 12:12 10°C: ZT0 n = 13, ZT4 n = 14, ZT8 n = 15, ZT12 n = 15, ZT16 =16, ZT20 n = 10.

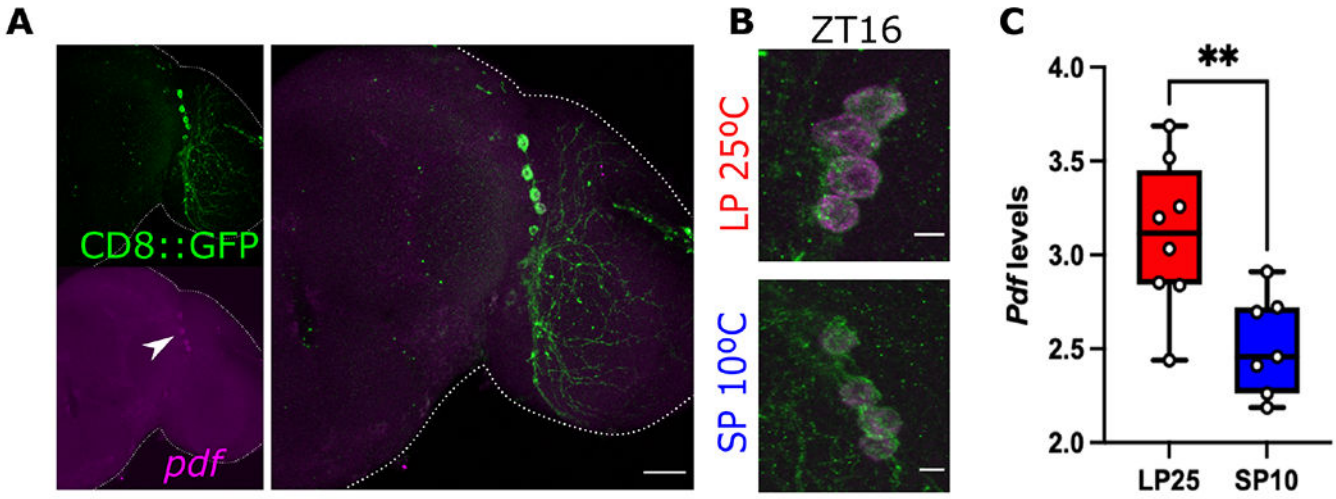

Figure 2. *Pdf* mRNA is sensitive to seasonal cues.

(A) *Pdf* mRNA (magenta) was detected using fluorescence in situ hybridization (FISH) in whole brains of flies entrained for 7 days to simulated-summer (LP at 25°C) or simulated-winter (SP at 10°C). CD8::GFP was expressed using the *Pdf-gal4* driver to detect the PDF-producing LNvs. (B) Representative images of LNvs of flies entrained to LP 25°C (top panel) or SP 10°C (bottom panel). (C) Quantification of the normalized intensity of the *Pdf* signal at ZT16 is compared between conditions. Unpaired t-test, ** p <0.01. Number of brains imaged were LP25 n = 8, SP10 n = 7 brains. Scale bar in A is 25 μm and 5 μm in B. See also Figure S1 and Table S1.

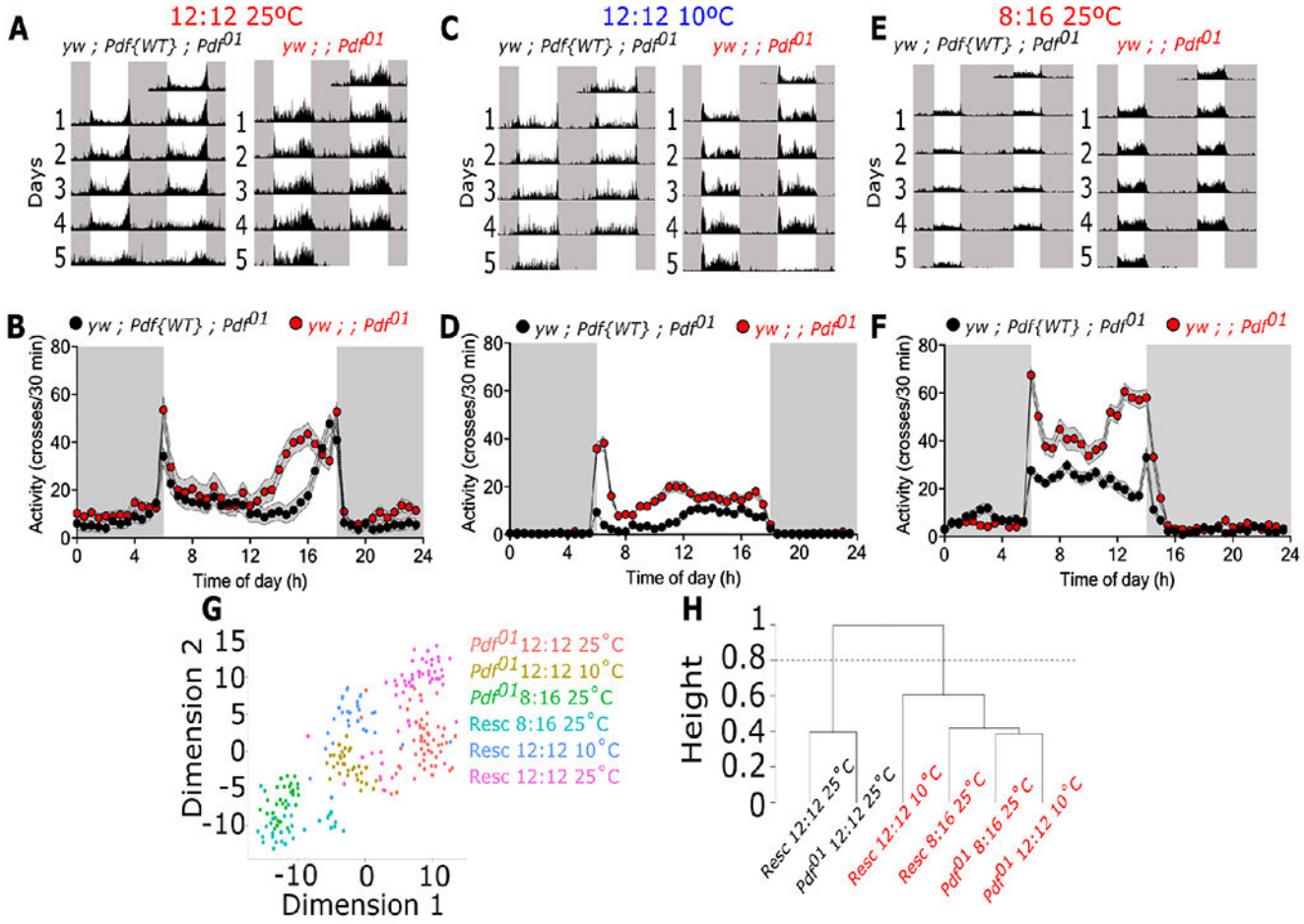

Figure 3. Locomotor adaptation to photoperiod and temperature in *Pdf*-null mutants.

Locomotor activity was monitored in *Pdf*-null mutants (*yw ; Pdf*^{01}) and in flies expressing a wild-type copy of *Pdf* (genomic rescue, *yw ; Pdf{WT} ; Pdf*^{01}) subjected to (A-B) 12:12 LD at 25°C, (C-D) 12:12 LD at 10°C, or (E-F) 8:16 LD at 25°C. (G) Variance in locomotor activity under these environmental conditions as tSNE of the normalized locomotor activity for Rescue (Resc) and the mutant (*Pdf*^{01}). Each dot represents an individual fly. (H) Hierarchical clustering of the normalized locomotor activity. Arbitrary cut of the tree at 0.8 (y-axis) generates two distinct groups denotated as black and red labels. White boxes represent lights-on while black boxes represent lights-off in panels A-F. Data were analyzed using a two-way ANOVA with Bonferroni's multiple comparison test. Number of flies used were *yw ; Pdf{WT} ; Pdf*^{01} 12:12 25°C n = 56, *yw ; Pdf{WT} ; Pdf*^{01} 8:16 25°C n = 30, *yw ; Pdf{WT} ; Pdf*^{01} 12:12 10°C n = 30, *yw ; ; Pdf*^{01} 12:12 25°C n = 55, *yw ; ; Pdf*^{01} 8:16 25°C n = 31, *yw ; ; Pdf*^{01} 12:12 10°C n = 32.

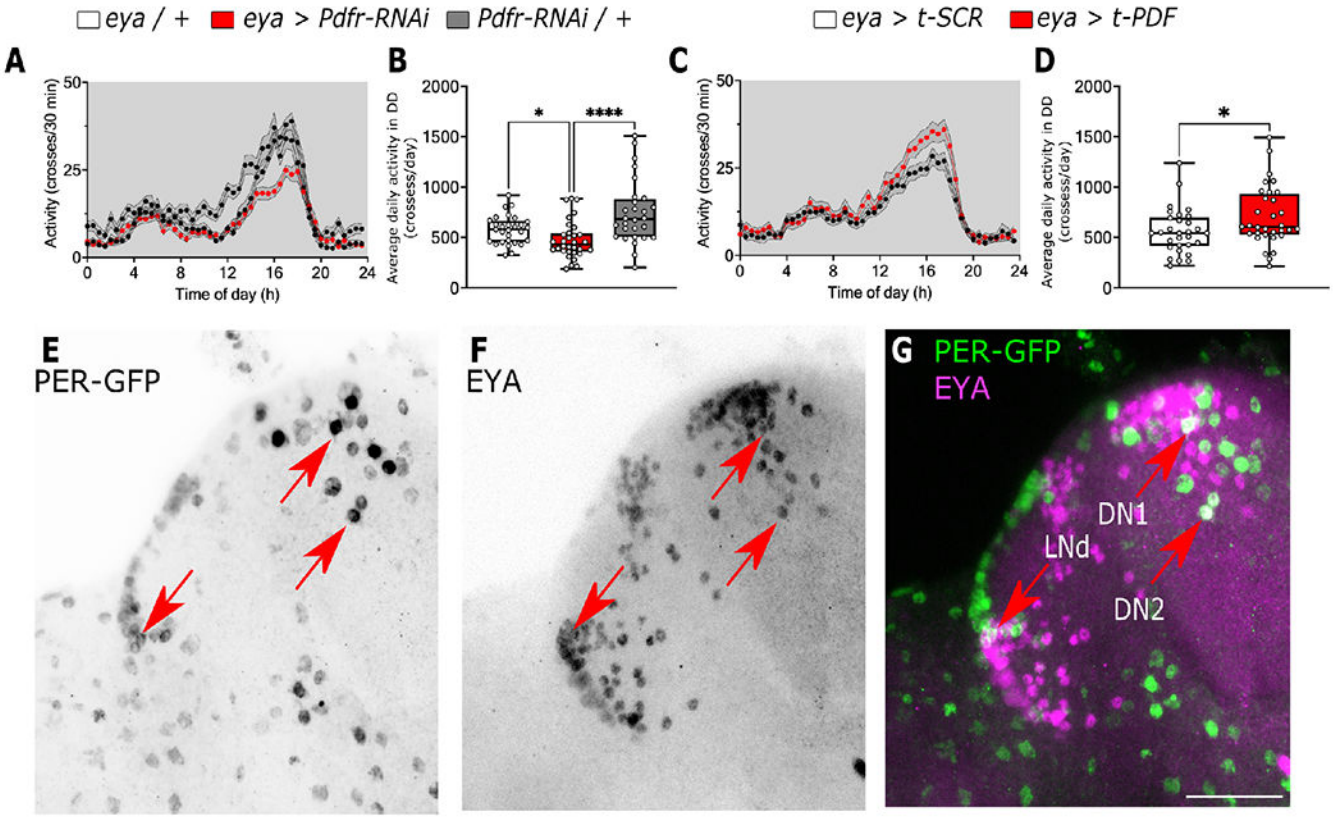

Figure 4. PDF modulates overall locomotion through *eya*+ cells.

(A-B) Average locomotor activity of flies in constant darkness at 25°C where the PDF receptor was knocked down in *eya*+ cells (*eya > Pdfr-RNAi* red line and box) compared to controls (*eya* / + and *Pdfr-RNAi* / +, black and gray lines, respectively). (C-D) Average locomotor activity of flies where a membrane tethered version of PDF was expressed in *eya*+ cells (*eya > t-PDF* red line and box) compared to the expression of a scrambled version of the peptide (*eya > t-SCR* black line and box). (E-G) Confocal images of fly brain expressing endogenous GFP tagged PER (green) and stained against EYA (magenta). Red arrows points DN1, DN2 and LNd clock populations. Scale bar is 25 μm. Data in B were analyzed with Kruskal-Wallis test followed by Dunnett's multiple comparison test, Mann-Whitney in D. Number of flies used were *eya / +* n = 29, *eya > Pdfr-RNAi* n = 32, *Pdfr-RNAi / +* n = 28, *eya > t-SCR* n = 31, *eya > t-PDF* n = 31, *eya / +* n = 30. See also Figures S2 and S3.

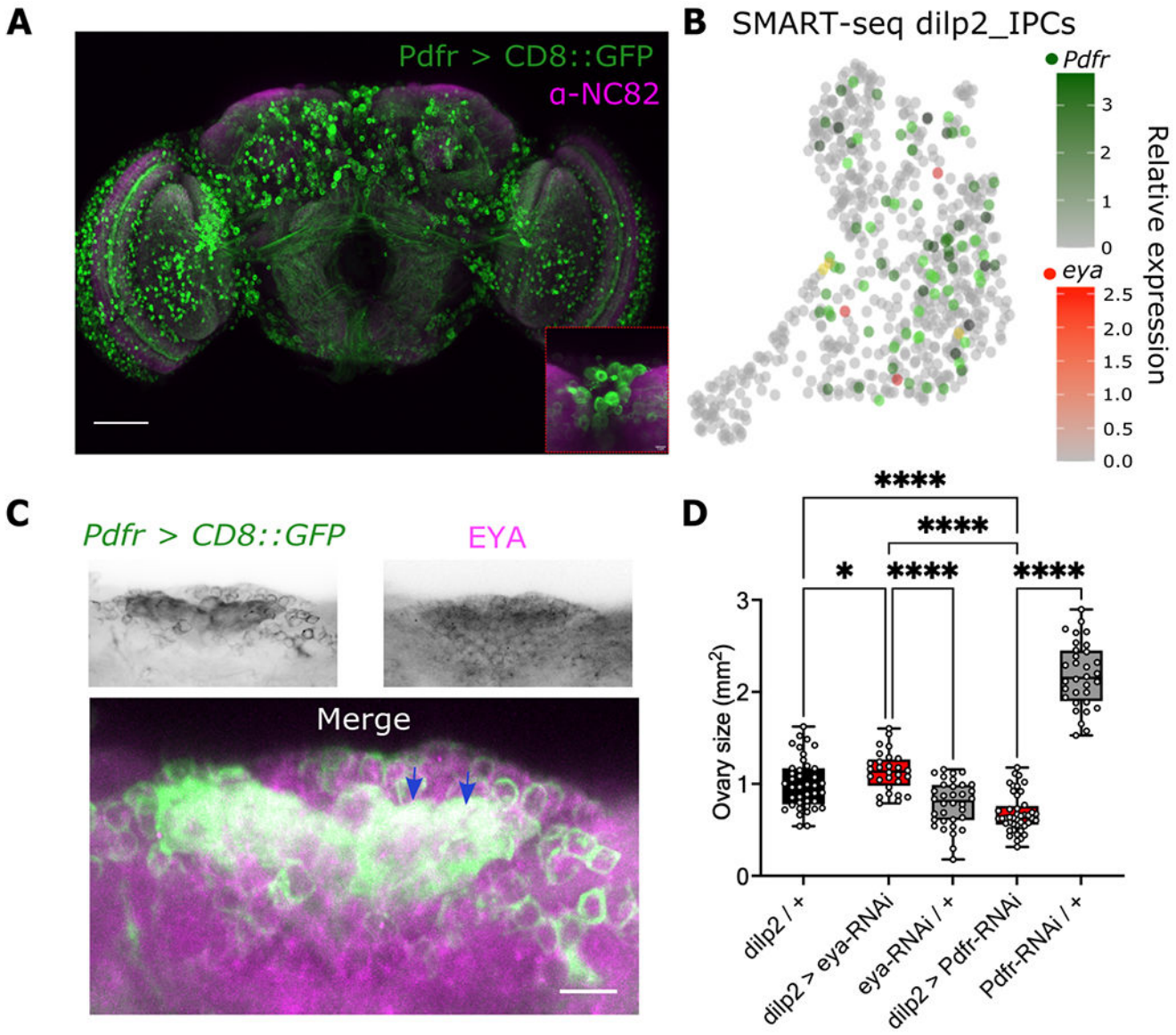

Figure 5. PDF and EYA have opposite effects in the IPCs to modulate ovary size under summer-like conditions (16:8 LD at 25°C)

(A) Expression of CD8::GFP was driven in the *Pdfr+* cells using a *Pdfr-gal4* driver. Nc82 antibody was used as counterstaining. Expression of CD8::GFP is observed in several segments of the brain, including the *pars intercerebralis*, containing the IPCs (inset). Scale bar is 50μm. (B) SMART-seq dataset from *dilp2+* isolated IPCs from Fly Cell Atlas[53] as UMPA, colored by *Pdfr* (green) and *eya* (red) expression. Coexpression is shown as yellow. Color bar denotes the relationship between color intensity and relative expression levels. (C) EYA staining (upper right panel) in brains of flies expressing CD8::GFP in the *Pdfr+* cells (*Pdfr > CD8::GFP*, upper left panel). Merged image is observed in the bottom panel. Scale is 5 μm. (D) Comparison of ovary size in mm^2 while knocking down *eya* (*dilp2 > eya-RNAi*) or knocking down *Pdfr* (*eya > Pdfr-RNAi*) compared to genetic controls (black and grey boxes). Data was analyzed using a one-way ANOVA followed by Holm-šidák's

multiple comparison test. Number of flies used were *dilp2 / +* n = 40, *dilp2 > eya-RNAi* n = 28, *eya-RNAi / +* n = 34, *dilp2 > Pdfr-RNAi* n = 45, *UAS-Pdfr-RNAi / +* n = 32.

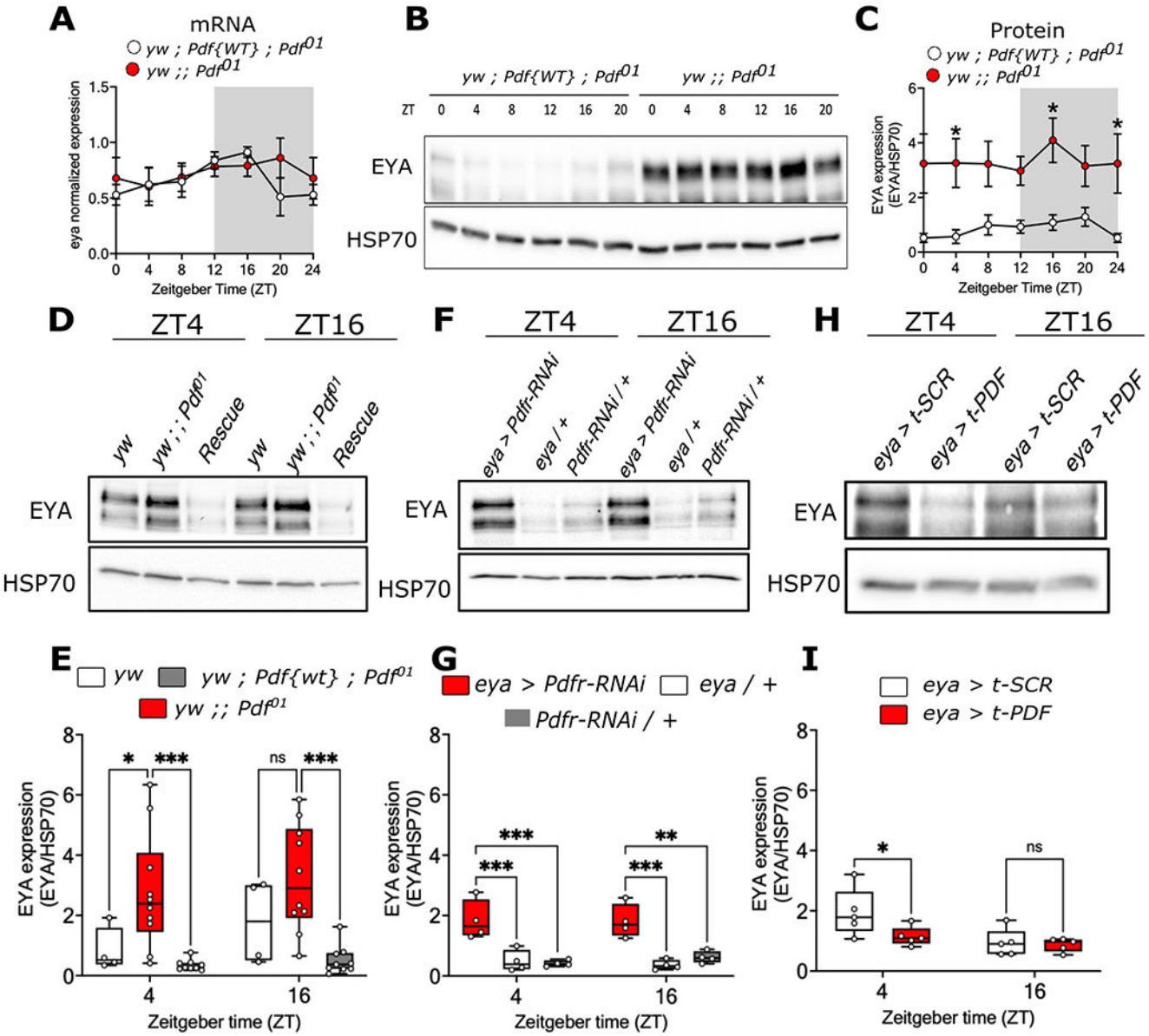

Figure 6. PDF modulates EYA protein but not *eya* mRNA expression.

(A) *eya* mRNA daily oscillations in *Pdf*-null mutants (*yw ; ; Pdf*^{01} flies, red dots, RAIN p = 0.833) and in flies expressing a *Pdf* genomic rescue (*yw ; Pdf{WT} ; Pdf*^{01}, white dots, RAIN p = 0.0078) in 12:12 LD cycles at 25°C. (B) Representative western blot and (C) quantification of EYA levels in whole-head lysates from *Pdf* null-mutant (red dots, RAIN p = 0.677) and in the genomic rescue (white dots, RAIN p = 0.039) at ZT0, 4, 8, 12, 16 and 20 in 12:12 LD 25°C cycles. (D) Representative western blot and (E) quantification of EYA levels from whole head lysates of *yw* (genetic control, white boxes), *Pdf-null* mutants (red boxes) and the genomic rescue (grey boxes) at ZT4 and ZT16 in 12:12 LD 25°C condition. (F) Representative western blot and (G) quantification of EYA levels in head lysates of flies where the PDF receptor was knocked down in *eya+* cells (*eya > Pdfr-RNAi*, red boxes) and controls (*eya* / + and *Pdfr-RNAi* / +, white and grey boxes, respectively) at ZT4 and ZT16.

(H) Representative western blot and (I) quantification of EYA levels in flies expressing a membrane-tethered version of PDF in *eya+* cells (*eya > t-PDF*, red boxes) compared to a scrambled peptide as control (*eya > t-SCR*, white boxes) at ZT4 and ZT16. Data were analyzed using a two-way ANOVA followed by Tukey's post hoc test in B and C, and šídák's multiple comparison test in E, G and I. HSP70 was used for normalization in all cases. n > 3 biological replicates, each consisting of around 50 flies for each genotype.

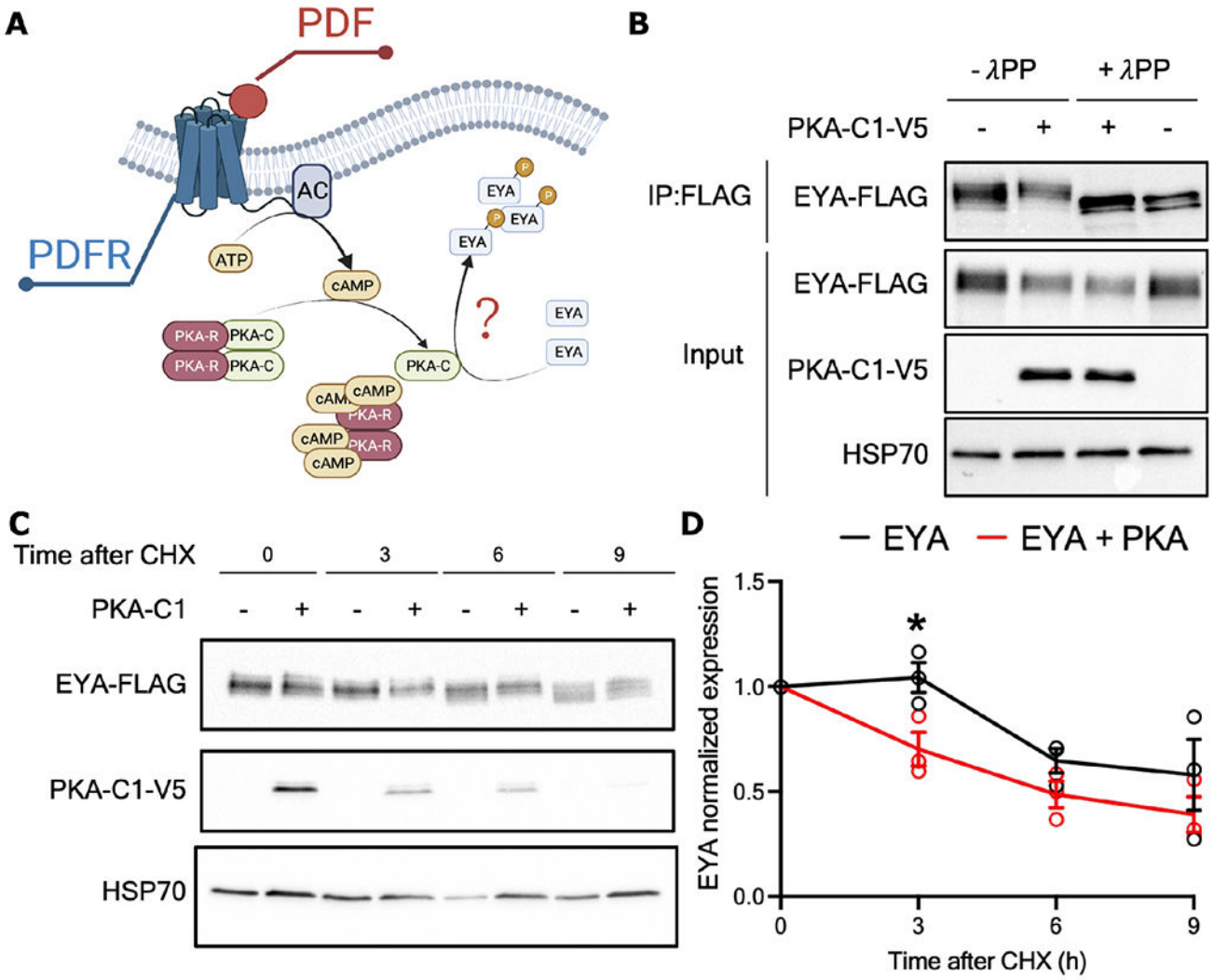

Figure 7. PKA phosphorylates EYA and mediates its degradation

(A) PDF receptor triggers the activation of adenylate cyclase (AC) which produces cAMP. The binding of cAMP to the regulatory subunits of the protein kinase A (PKA-R) releases the catalytic subunits of the kinase (PKA-C) permitting their action. EYA has potential sites for PKA phosphorylation. (B) *Drosophila* S2 cells co-expressing EYA-FLAG and the active C1 domain of PKA tagged with V5 (PKA-C1-V5 + condition) or EYA alone. Samples were then subjected to phosphatase treatmet (+λPP) and compared to samples that were mock treated (−λPP). Immunoprecipitated EYA was detected using α-FLAG in the input. α-V5 and α-HSP70 were used to detect PKA-C1 and HSP70 (n>3, representative image is shown). (C) Representative western blot of a CHX chase assay in S2 cells co-expressing EYA-FLAG alone or with PKA-C1-V5. (D) Quantification showing the rates of EYA degradation in absence (black line) or presence (red line) of PKA-C1. Data analyzed with two-way ANOVA with Holm-šídák's multiple comparison test. Each dot represents an independent experiment (n = 3, * $p<0.05$).

Key resources table

REAGENT or RESOURCE	SOURCE	IDENTIFIER
Antibodies		
Mouse monoclonal anti-PDF (clone C7-C)	Developmental Studies Hybridoma Bank	RRID: AB_760350 and AB_2315084
Mouse monoclonal anti-EYA (clone 10H6)	Developmental Studies Hybridoma Bank	RRID: AB_528232
Mouse monoclonal anti-BRP (nc82)	Developmental Studies Hybridoma Bank	RRID: AB_2314866
Chicken Polyclonal anti-GFP	Invitrogen	Cat#A10262; RRID: AB_2534023
Sheep anti-mouse IgG-HRP	GE Healthcare	Cat#NA931; RRID: AB_772210
Mouse monoclonal anti-V5	Thermo Fisher Scientific	Car#R960-25; RRID: AB_2556564
Mouse monoclonal anti-FLAG M2	Sigma-Aldrich	Cat# F3165; RRID: AB_259529
Goat Anti-mouse IgG Alexa647	Cell Signaling	Cat#4410; RRID: AB_1904023
Goat Anti-chicken IgG Alexa488	Thermo Fisher Scientific	Cat#A-11039; RRID: AB_2534096
Bacterial and virus strains		
Biological samples		
Chemicals, peptides, and recombinant proteins		
Schneider's *Drosophila* Medium	Thermo Fisher Scientific	Cat#21720-024
Fetal Bovine Serum	VWR	Cat# 97068-085
Penicillin/streptomycin	Thermo Fisher Scientific	Cat#15-140-148
Trypsin/EDTA	Thermo Fisher Scientific	Cat#25300-062
TRI regent	Sigma-Aldrich	Cat#T9424
Aprotinin	Sigma-Aldrich	Cat#A1153
Leupeptin	Sigma-Aldrich	Cat#L2884
Pepstatin A	Sigma-Aldrich	Cat#P5318
SIGMAFAST™ Protease Inhibitor Cocktail, EDTA-FREE	Sigma-Aldrich	Cat#S8830
ANTI-FLAG M2 Affinity Gel	Sigma-Aldrich	Cat#A2220
PhosSTOP	Sigma-Aldrich	Cat#4906845001
Normal Goat Serum	Jackson Immunoresearch	Cat#005-000-121
λ-Phosphatase	NEB	Cat#P0753S

REAGENT or RESOURCE	SOURCE	IDENTIFIER
SsoAdvanced SYBR green supermix	Bio-Rad	Cat#1725270
PBS 10X Rnase free	Invitrogen	Cat#AM9624
Nuclease-free water	Invitrogen	Cat#AM9932
Acetic Acid	Fisher	Cat#A38S-500
Sodium borohydride (99%)	Fisher	Cat#AC448481000
SSC (20X)	Fisher	Cat#AM9763
Hi-Di Formamide	Fisher	Cat#4311320
Triton X-100 nuclease-free	Fisher	Cat#AC327371000
Formamide (deionized)	Invitrogen	Cat#AM9342
Denhard's solution	Fisher	Cat#AAJ63135AD
tRNA from baker's yeast	Roche	Cat#10109495001
SDS 10%	Corning	Cat# 46-040-CI
UltraPure™ Salmon Sperm DNA Solution	Fisher	Cat# 15632011
4% PFA	EMS	Cat#157-4
Rnase AWAY	Thermo Fisher Scientific	Cat#7002PK
Ethanol (200 Proof)	Fisher	Cat#BP2818500
Critical commercial assays		
Superscript IV	Thermo Fisher Scientific	Cat#18091050
Effectene Transfection Reagents	QIAGEN	Cat#301425
Pierce Coomassie Plus Assay Reagents	Thermo Fisher Scientific	Cat#1856210
Deposited data		
Experimental models: Cell lines		
D. melanogaster: Cell line S2: S2-DRSC	Thermo Fisher Scientific	Cat#R69007
Experimental models: Fly lines		
D. melanogaster: w; Pdf-Gal4	Park et al. [53]	N/A
D. melanogaster: w; UAS-mCD8::GFP	Bloomington *Drosophila* Stock Center	#32184
D. melanogaster: yw; ; Pdf01	Bloomington *Drosophila* Stock Center	#26654
D. melanogaster: yw; Pdf-RescueB ; Pdf01	Renn et al. [46]	N/A
D. melanogaster: yw	Bloomington *Drosophila* Stock Center	#1495
D. melanogaster: w; ; eya-Gal4	Bloomington *Drosophila* Stock Center	#49292
D. melanogaster: w; UAS-Pdfr-RNAi	Bloomington *Drosophila* Stock Center	#38347
D. melanogaster: w; UAS-t-PDF	Bloomington *Drosophila* Stock Center	#81111
D. melanogaster: w; UAS-t-SCR	Bloomington *Drosophila* Stock Center	#81113
D. melanogaster: w; UAS-*eya*-RNAi	Vienna *Drosophila* Resource Center	#108071

REAGENT or RESOURCE	SOURCE	IDENTIFIER
D. melanogaster: w; *per-AID-GFP*	Chen et al.[61]	#108071
D. melanogaster: w; UAS-*eya*-RNAi	Vienna *Drosophila* Resource Center	#108071
D. melanogaster: Pdfr-Gal4 , w	Bloomington *Drosophila* Stock Center	#33070
D. melanogaster: w ; dilp2-Gal4 / Cyo	Bloomington *Drosophila* Stock Center	#37516
Oligonucleotides		
Primers for *eya*, see Methods details	This paper	N/A
Primers for *cbp20*, see Methods details	This paper	N/A
Library for *Pdf* detection, see Table S1	Long et al.[82]	N/A
Recombinant DNA		
Plasmid: pMT-V5	Thermo Fisher	Cat#V412020
Plasmid: pMT-PKA-C1-V5	This Paper	N/A
Plasmid: pAc-*eya*-3XFLAG-6XHis	Abrieux et al.[24]	N/A
Software and algorithms		
Fiji ImageJ (used for analysis of immunofluorescence microscopy images)	NIH Image	https://fiji.sc
GraphPad Prism 8 for Mac OS X	GraphPad Software	https://graphpad.com
Excel	Microsoft	Version 16.67
R	R Core Team	Version 4.0.3
RStudio	PBC	Version 2022.07.2
CircaCompare	Parsons et al.[55]	Release 0.1.1
RAIN	Thaben & Westermark[56]	Release 3.16
Other		